CAIT-UTC-NC47

National University Transportation Consortium: A Speaker Recognition Based Damage Detection

FINAL REPORT
August 2018

Submitted by:

Raimondo Betti, Ph.D.
Department of Civil Engineering and Engineering Mechanics
Columbia University

External Project Manager

Dyab Khazem
Engineering Manager and Technical Director
Parsons Transportation Group

In cooperation with

Rutgers, The State University of New Jersey
And
U.S. Department of Transportation
Federal Highway Administration

Disclaimer Statement

The contents of this report reflect the views of the authors, who are responsible for the facts and the accuracy of the information presented herein. This document is disseminated under the sponsorship of the Department of Transportation, University Transportation Centers Program, in the interest of information exchange. The U.S. Government assumes no liability for the contents or use thereof.

The Center for Advanced Infrastructure and Transportation (CAIT) is a National UTC Consortium led by Rutgers, The State University. Members of the consortium are the University of Delaware, Utah State University, Columbia University, New Jersey Institute of Technology, Princeton University, University of Texas at El Paso, Virginia Polytechnic Institute, and University of South Florida. The Center is funded by the U.S. Department of Transportation.

1. Report No.	2. Government Accession No.	3. Recipient's Catalog No.
CAIT-UTC-NC47		

4. Title and Subtitle	5. Report Date
National University Transportation Consortium: A Speaker Recognition Based Damage Detection	August 2018
	6. Performing Organization Code CAIT/Columbia University
7. Author(s) Raimondo Betti, Ph.D.	8. Performing Organization Report No. CAIT-UTC-NC47
9. Performing Organization Name and Address Columbia University Department of Civil Eng. and Eng. Mech 500 W. 120th Street, NY, NY 10027	10. Work Unit No. 11. Contract or Grant No. DTRT13-G-UTC28
12. Sponsoring Agency Name and Address Center for Advanced Infrastructure and Transportation Rutgers, The State University of New Jersey 100 Brett Road Piscataway, NJ 08854	13. Type of Report and Period Covered Final Report 9/1/16 – 6/30/18 14. Sponsoring Agency Code

15. Supplementary Notes
U.S. Department of Transportation/OST-R
1200 New Jersey Avenue, SE
Washington, DC 20590-0001

16. Abstract
In this study, an adaptation of Mel-Frequency Cepstral Coefficients as damage sensitive features for structural health monitoring of civil structures was addressed. Typically used in speaker recognition methodologies, these indices offer an extremely easy extracting process with a few user-defined parameters and a low computational burden and they have been shown to be an effective alternative to other features for damage detection problems. To remove environmental effects from the coefficient estimation, a technique called "Cointegration", quite popular in econometrics, has been applied. Two study cases were presented: 1) a numerical simulation of a cantilever beam subject to environmental variations both in undamaged as well as damaged conditions, and 2) the benchmark case of the Z24 bridge, a structure in Switzerland that was recently demolished and that was fully instrumented, during operational conditions as well as during demolition.
From the results of this study, it appears that the following conclusions can be drawn: 1) the cepstral coefficients have the potential to become quite useful damage sensitive features that can be used on bridge structures: they are compact features, easy to obtain, and require little input from the user, and 2) the cointegration technique appears to be a very effective technique to remove non-stationary effects such as those induced by the environment temperature. As shown in this report, the analyses conducted on data from the tests run on the Z24 bridge show great potential for both techniques and warrants further investigation.

17. Key Words	18. Distribution Statement
Damage detection, cepstral coefficients, cointegration	

19. Security Classification (of this report)	20. Security Classification (of this page)	21. No. of Pages	22. Price
Unclassified	Unclassified	Total #38	

A Speaker Recognition Based Damage Detection

Raimondo Betti

August 26, 2018

Abstract

Vibration based damage detection methods are typically used in Structural Health Monitoring to keep track of the deterioration and identify the presence of damage in civil structures like bridges and buildings. The basic idea behind such methods is to monitor the variational pattern of certain features (e.g. natural frequencies, mode shapes, etc.) extracted from the measured structural response. The performance of these approaches predominantly depends on how well these features reflect the actual condition of the structure. In fact, modal parameters, such as natural frequencies and mode shapes are commonly used in monitoring the performance of bridges and buildings: however, in assessing the damage of such structures, these features could be misleading in pointing out the integrity status of the structure since they are highly influenced by the usual fluctuations in environmental and operational conditions. The effects of environmental and operational conditions could overshadow the occurrence of deterioration and damage, invalidating the purpose of the investigation.

Recently an adaptation of Mel-Frequency Cepstral Coefficients as damage sensitive features for structural health monitoring of civil structures was addressed. Typically used in speaker recognition methodologies, these indices offer an extremely easy extracting process with a few user-defined parameters and a low computational burden and they have been shown to be an effective alternative to other features for damage detection problems.

This report investigates the dependency of cepstral coefficients from the mechanical properties of structures and in detail on how they behave when these properties vary. In Chapter 1 the extraction procedure which needs to be followed to compute these features is presented. After introducing the theoretical background a brief introduction is made of the cointegration technique, which is a methodology that can be used to remove the environmental trend from monitoring data. In Chapter 3 and Chapter 4 two study cases are presented: 1) a numerical simulation of a cantilever beam subject to environmental variations both in undamaged as well as damaged conditions, and 2) the benchmark case of the Z24 bridge, a structure in Switzerland that was recently demolished and that was fully instrumented, during operational conditions as well as during demolition.

Contents

Chapter 1

Cepstral Coefficients

1.1 Introduction

The Mel-Frequency Cepstral Coefficients are features commonly used in the field of speaker and speech recognition. These are features that are extracted from the recorded voice signal and are used to characterize the "structure" of the vocal apparatus of an individual. Even though they are linked to the mechanical properties of a system, they are substantially different from other features generally in Structural Health Monitoring problems, such as modal frequencies or mode shapes, as they allow for consideration of the response property in both the frequency and time domain simultaneously. Since structural damage alters the structural response, it is reasonable to expect that the cepstral coefficients will also experience a variation and so, by tracking their variation over time, it will be possible to detect the occurrence of damage, its significance and the location of the occurrence.

The cepstrum of a signal $x(t)$ is defined as the inverse Fourier transform of the log-spectrum of $x(t)$. Originally the cepstrum was born with the aim of finding a procedure able to filter the effects of echoes from time series and it was firstly introduced by Bogert [1] and his colleagues at Bell Laboratories in 1963. The discrete-time formulation of the cepstrum and of its complex counterpart, the complex cepstrum, was lately addressed by Schafer and Oppenheim [2]. A compact version of the cepstrum was proposed in 1980 by Davis and Mermelstein [3], who suggested the use of the Mel-spectrum, named after the Melody scale, to get the cepstral representation of speech signals. The discrete set of coefficients extracted from the sampled speech signal were called Mel-Frequency Cepstral Coefficients. It is noteworthy that such representation of the cepstral features is a compact version of the real cepstrum, which preserve only information on the magnitude of the log-spectrum, while the information on the phase are lost.

The first application of these coefficients for civil engineering applications was given by Zhang et al. [4], who used MFCCs to detect concrete delamination on a bridge deck by analyzing the MFCCs extracted from records of the impact sound produced by impacting the surface of the concrete slab with a steel bar. Recently an adaptation of Mel-Frequency Cepstral Coefficients as damage sensitive features feasible for SHM purposes was proposed by Balsamo and her colleagues [5]. These are the features herein explored, as their compactness and decorrelation characteristics make them particularly suited to be used as damage sensitive features. Moreover these coefficients require very low user expertise to be extracted and analyzed, making them particularly convenient for implementation into automatic structural health monitoring procedures. In this chapter, the extraction procedure of an adaptation of MFCC features to best fit the characteristics of structural response time histories is explored. These features are extracted directly from the time histories of the structural response and are used in a statistical pattern recognition approach to infer damage occurrence.

1.2 Feature selection

In the following block diagram, a schematic representation of the extraction process of the cepstral coefficients ($c[d]$) from a given data sequence ($x[n]$) is shown.

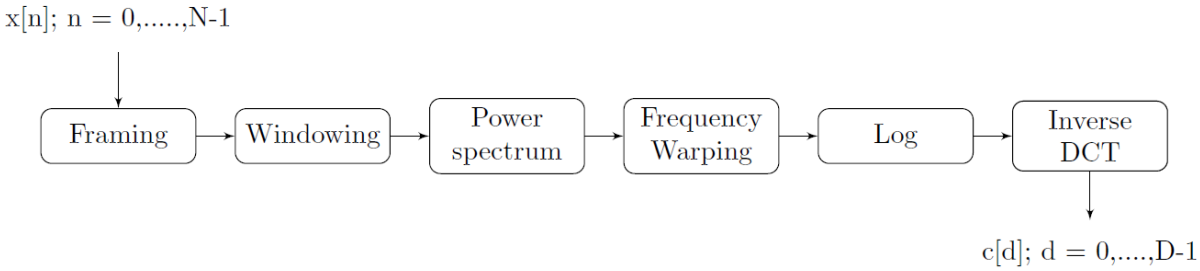

The extraction process of cepstral coefficients is extremely simple and has low computational requirements. The cepstral coefficients can be extracted from a sampled signal $x[n]$ applying the procedure defined in the flow chart in (1.2), the reader is referred to [5] for a detailed treatment of the subject.

This section focuses on the steps that need to be followed in order to extract the cepstral coefficients from a sampled time history. In order to simplify the description of the process, the extraction methodology is applied to the time-history of the acceleration response of a single degree-of-freedom system. This will allow us to highlight the cepstral coefficients are linked to the structural properties of the system.

The simulated system tested in this case is a 1-story shear-type system, modeled according to the common mass-spring-viscous damper chain. The baseline system is characterized by a stiffness, $k_0 = 6 \times 10^6$ N/m, and mass, $m_0 = 2 \times 10^3$ Kg. The energy dissipation properties of the system are modeled through the Rayleigh damping mechanism. The acceleration response to a white Gaussian noise input is simulated. The input time histories, of mean 0 and standard deviation 1, are 2 minutes long, sampled at 0.005 s (f_s=200 Hz). From an analysis of the power spectrum of the response, it is possible to see that the entire energy content is between 0 Hz and 50 Hz. Since this example is just to highlight the extraction of the cepstral coefficients of the structural response, no measurement noise is introduced in the signal.

1.2.1 Framing and Windowing

In the preliminary step, each one of the N_{th} recorded time histories is framed into N_{frames} segments (each segment is called "a frame"), which must be long enough so to be considered stationary. In each segment (or frame), $N_{samples}$ represents the number of samples or data points. Then, in order to reduce the riddle effects on the frame spectra due to the segmentation procedure (leakage phenomenon), non-rectangular windows (usually Hamming windows) are applied to each frame.

The Hamming window is by far the most popular window used in speech processing. One reason for the popularity of the Hamming window is the fact that its spectrum falls off rather quickly, so it allows for better isolation of the predominant frequencies. However, its, so called, side-lobes (higher harmonics) stay quite flat and they cover most of the spectrum. Equation 1.1 shows the expression for the k_{th} coeffcient of a K-point Hamming window:

$$w[k] = 0.54 - 0.46 \cos\left(\frac{2\pi k}{K}\right), \text{ for } \quad k = 0, ..., K-1 \tag{1.1}$$

In Figures 1.1, 1.2 and 1.3, the framing and windowing process for a single time history of the SDOF system under consideration are graphically presented.

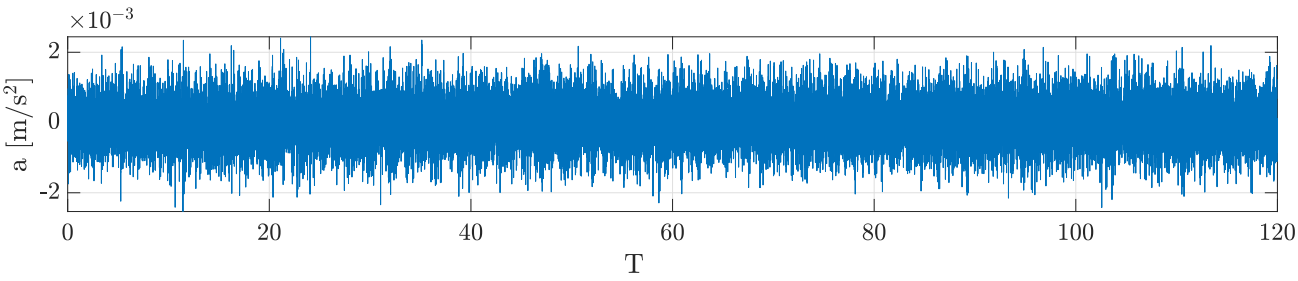

Figure 1.1: Acceleration Response

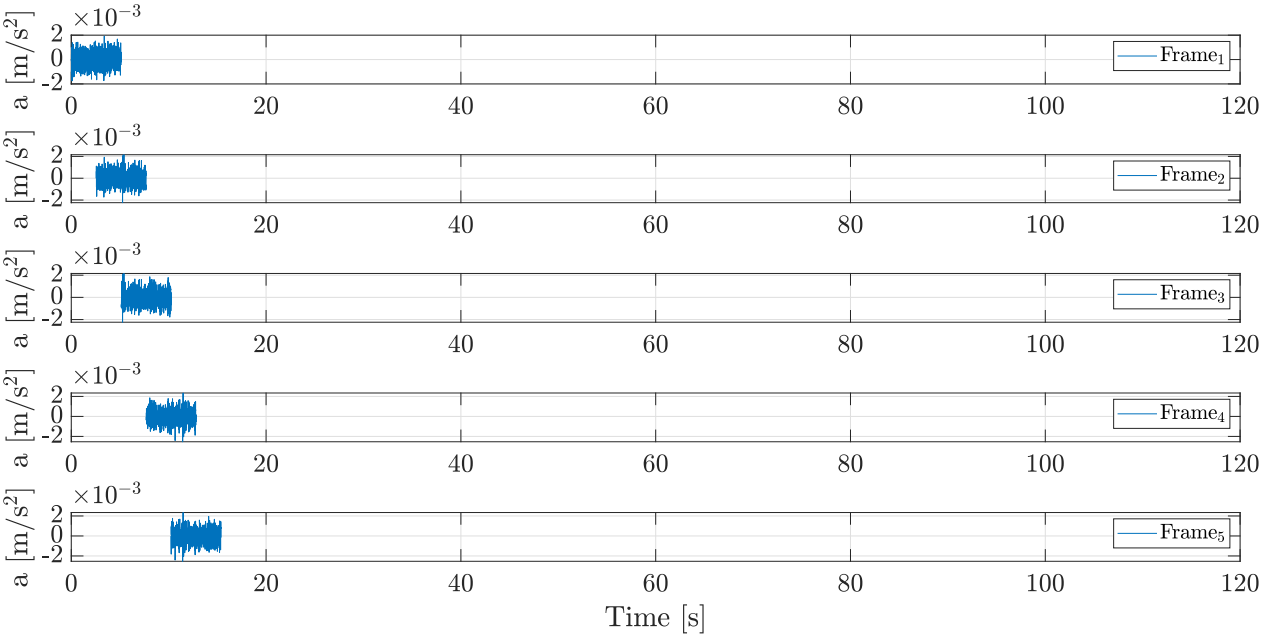

Figure 1.2: Framed Time History for the first 5 frames

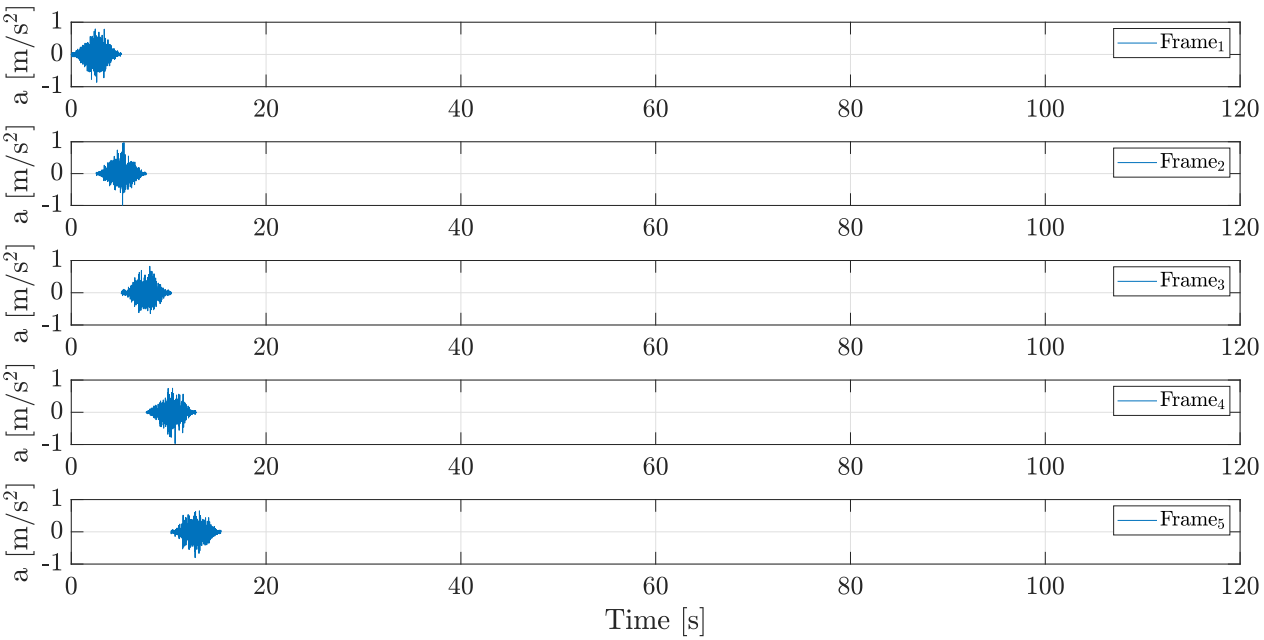

Figure 1.3: Windowed Framed Time History for the first 5 frames

Subsequently, applying the Discrete Fourier Transform (DFT) the power spectrum is evaluated for each frame.

1.2.2 Frequency warping

In order to emphasize the parts of the spectrum that are more likely to represent the structural behavior, a frequency warping procedure is performed. Such a procedure allows to modify and scale the linear frequency scale with the objective of weighing more the area of the spectrum with the greatest energy content. The new modified frequency scale and the linear frequency scale are almost equivalent up to a cutoff frequency f_c, after which their relation becomes logarithmic. This approach is quite similar to the one commonly done in speaker recognition but with a different cutoff frequency: in fact, this new scale mimics the trend of the Mel-scale used in acoustics, but working on a frequency range compatible with structural problems. This cutoff parameter is

defined by the user: in this specific example, the value of f_c is set equal to 11 (Hz.).

If N_{frames} is the number of frames obtained from one time history, at the end of this first stage for each of the N_{th} realization, there will be $N_{samples} \times N_{frames}$ response windowed segments. Averaging the spectra of all such segments results in what will be referred to as an *average spectrum*. The average spectrum highlights the frequency range within which the greatest frequency content is observable. The cutoff frequency is then chosen as the upper bound of the portion of the averaged spectrum (Fig. 1.4).

$$\tilde{f} = f_c \log_2(1 + \frac{f}{f_c}) \tag{1.2}$$

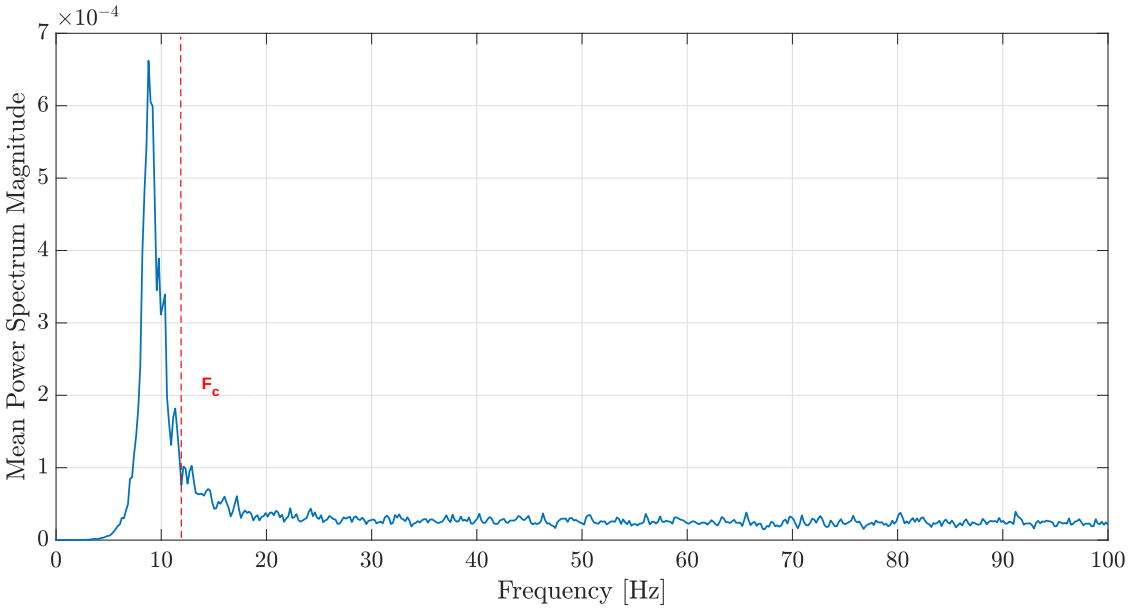

Figure 1.4: Averaged PS on all the frames

Once the average spectrum is computed and the frequency rage is scaled accordingly, then the so-called "frequency warping" begins. The frequency warping step is performed by grouping together the Power Spectral values into M critical bands and weighting each group by a triangular weighting function. The number of critical bands, M, is set equal to $3ln(f_s)$, where ln() represents the natural logarithm operation, while f_s is the sampling frequency: this relationship is quite common in the speaker recognition research field and can be adopted also for structural problems.

The triangular filters are constructed such that their centers are equally spaced on the frequency scale ($\tilde{f}$), given in Eq.(1.2), with each filter being symmetric with respect to its center (see Fig. 1.5).

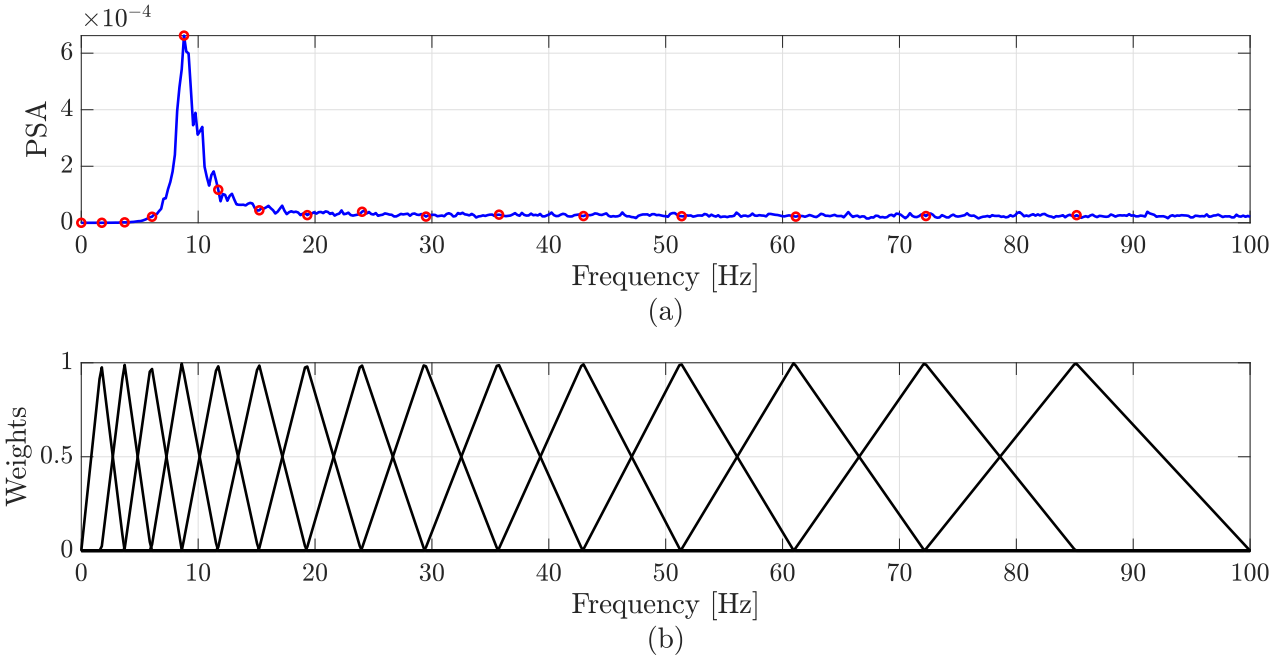

Figure 1.5: Power Spectrum Amplitude and Weights of the triangular filter

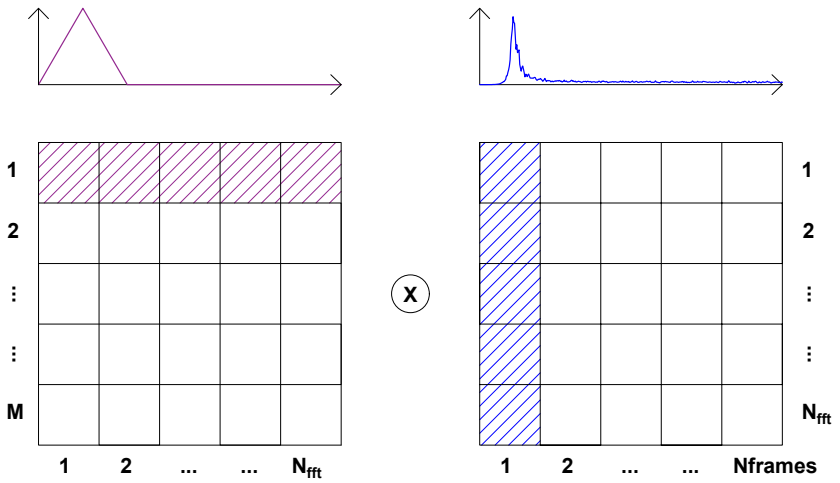

Figure 1.6: Multiplication of Power Spectrum Amplitude and Weights of the triangular filter

Consequently, the power spectrum of each frame is weighted by multiplying it by the triangular filter corresponding to each m_{ith} frequency band (Fig. 1.7). After that, each contribution coming from this multiplication is summed up leading to the matrix H of dimensions $M \times N_{frames}$.

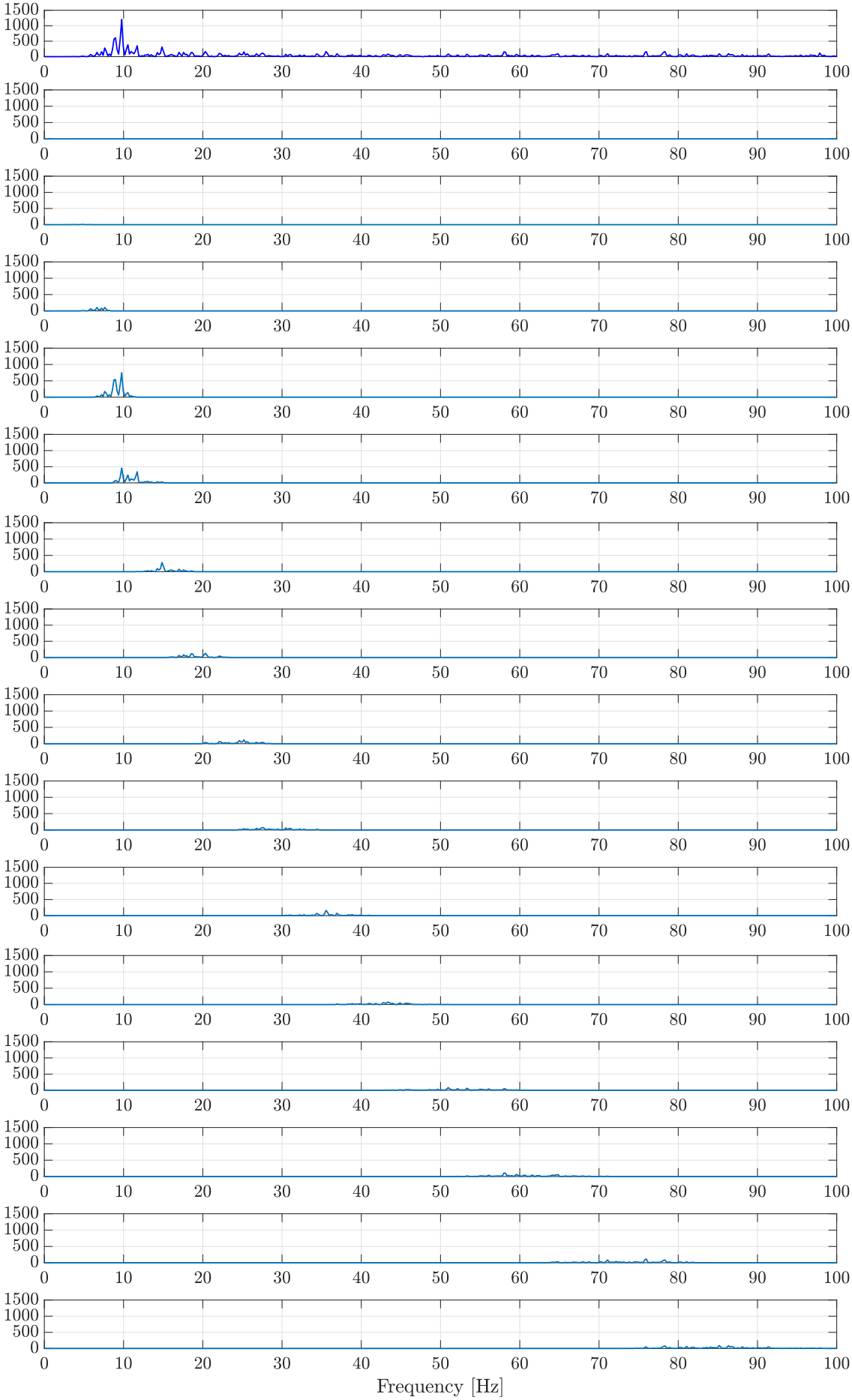

Figure 1.7: Multiplication of Power Spectrum Amplitude and Weights of the triangular filter

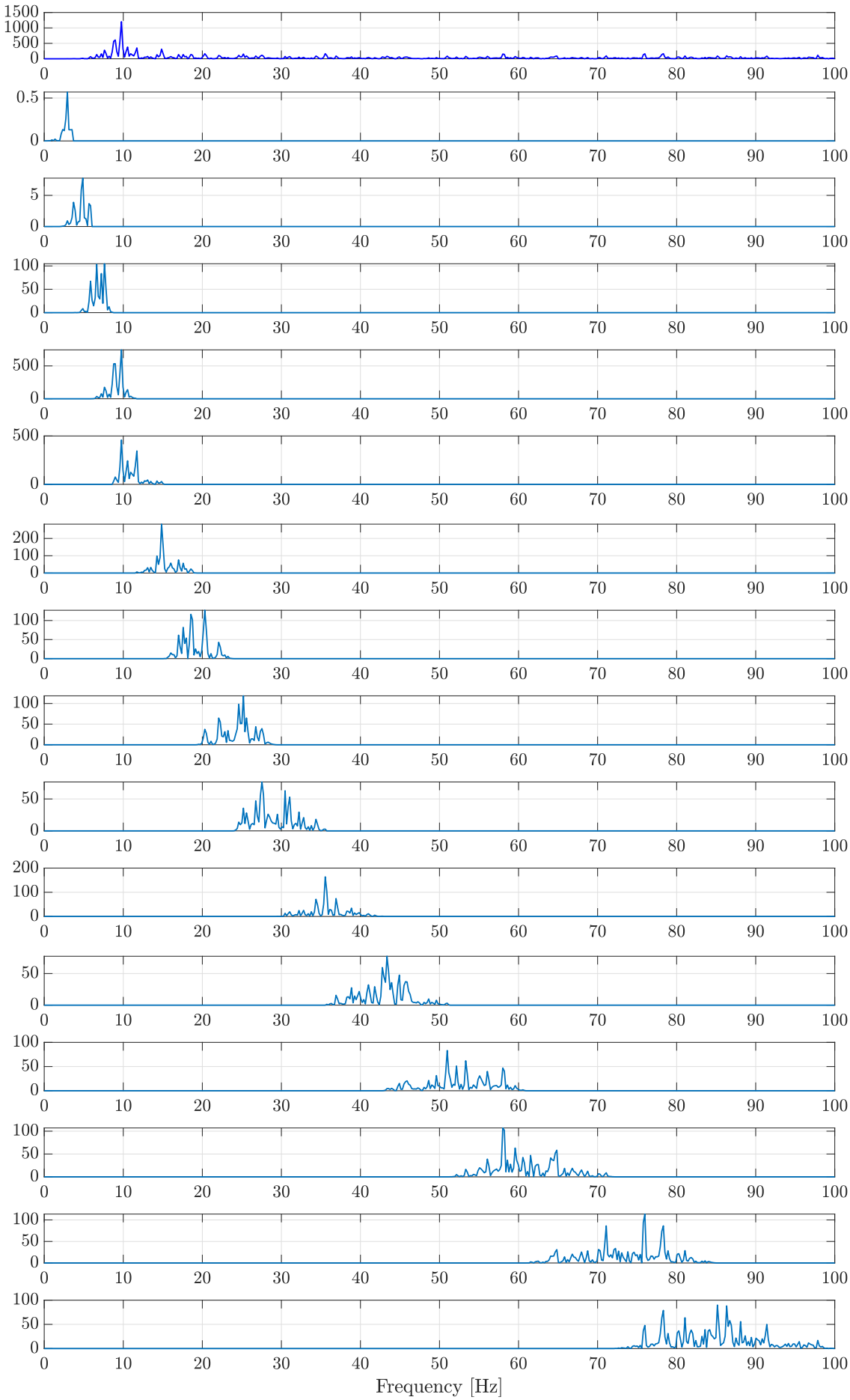

Figure 1.8: Multiplication of Power Spectrum Amplitude and Weights of the triangular filter

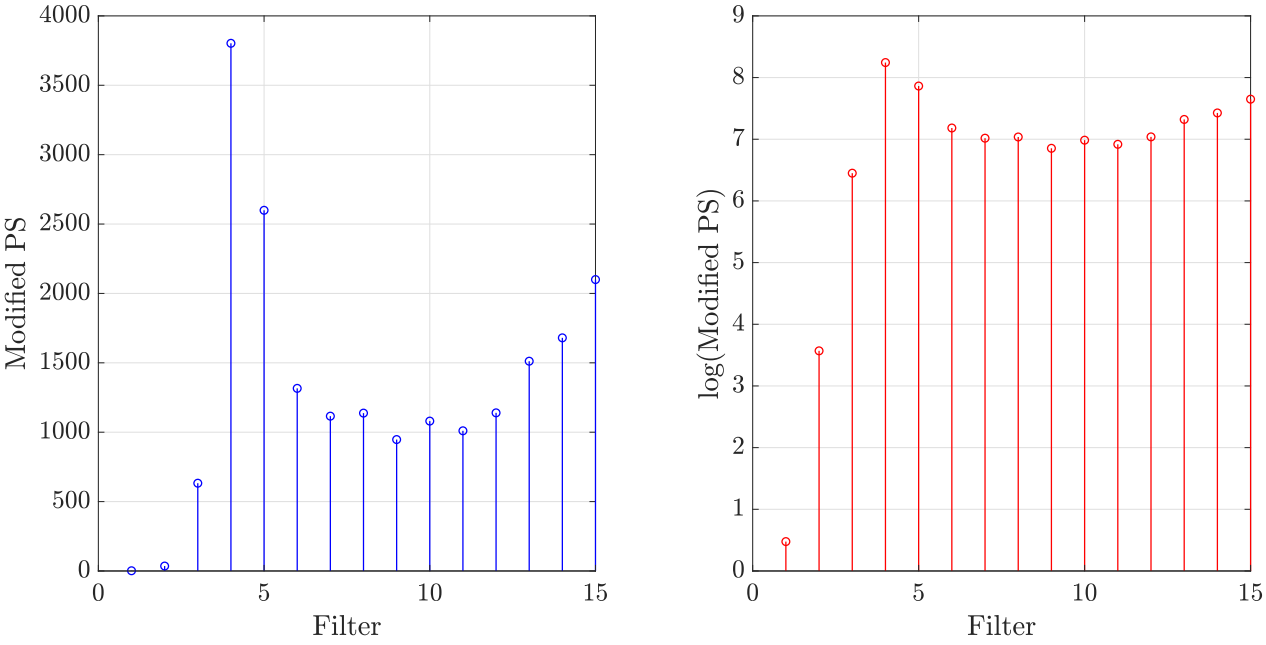

Figure 1.9: Modified PS and Log Modified PS for frame 1 of the first degree of freedom

1.2.3 Extraction of Cepstral Coefficients (CC)

The cepstrum coefficients extraction procedure is completed applying to the logarithm of the modified spectra an D-points Inverse Discrete Cosine Transform (IDCT) so to obtain:

$$c[d,k] = \sum_{m=0}^{M-1} a_m \ln(H[m,k]) cos[\frac{\pi(2d+1)m}{2M}] \qquad for\ d = 0,...,D-1 \quad for\ k = 1,...,N_{frames} \tag{1.3}$$

where a_m is equal to $\frac{1}{M}$, for m=0, and to $\frac{2}{M}$ otherwise. $H[m]$ represents the mth point of the modified spectrum, where m=0,...,M-1 while $c[d]$ is the d_{th} cepstral coefficient, which could be collected in a coefficient vector for each k_{th} frame $\mathbf{c}(k) \in \mathbb{R}^{D\times 1}$.

From a purely educational point of view, we could compute the coefficients of IDCT independently for each cepstral coefficients (Fig. 1.11) in order to better appreciate how these coefficients modify the different frequency contribution of the newly modified log spectrum (Fig. 1.10).

$$c_{IDCT}[d] = \sum_{m=0}^{M-1} a_m cos[\frac{\pi(2d+1)m}{2M}] \qquad for\ d = 0,...,D-1 \tag{1.4}$$

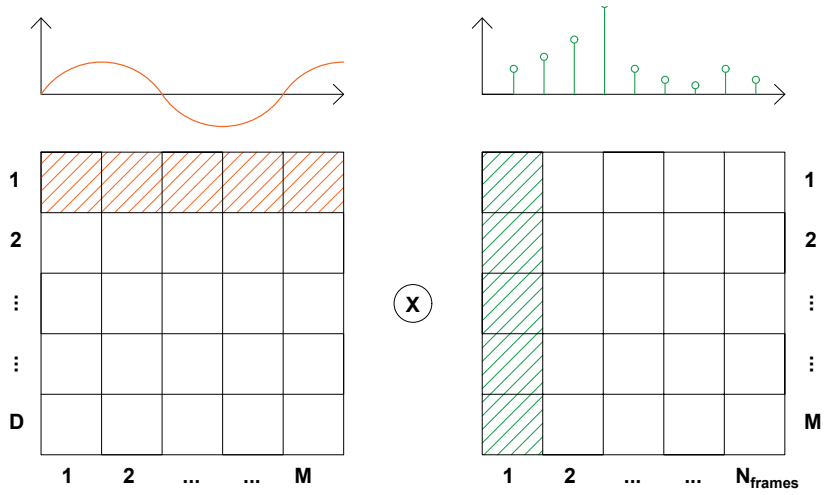

Figure 1.10: Multiplication of DCT coefficients by the log of the modified spectrum per each frame

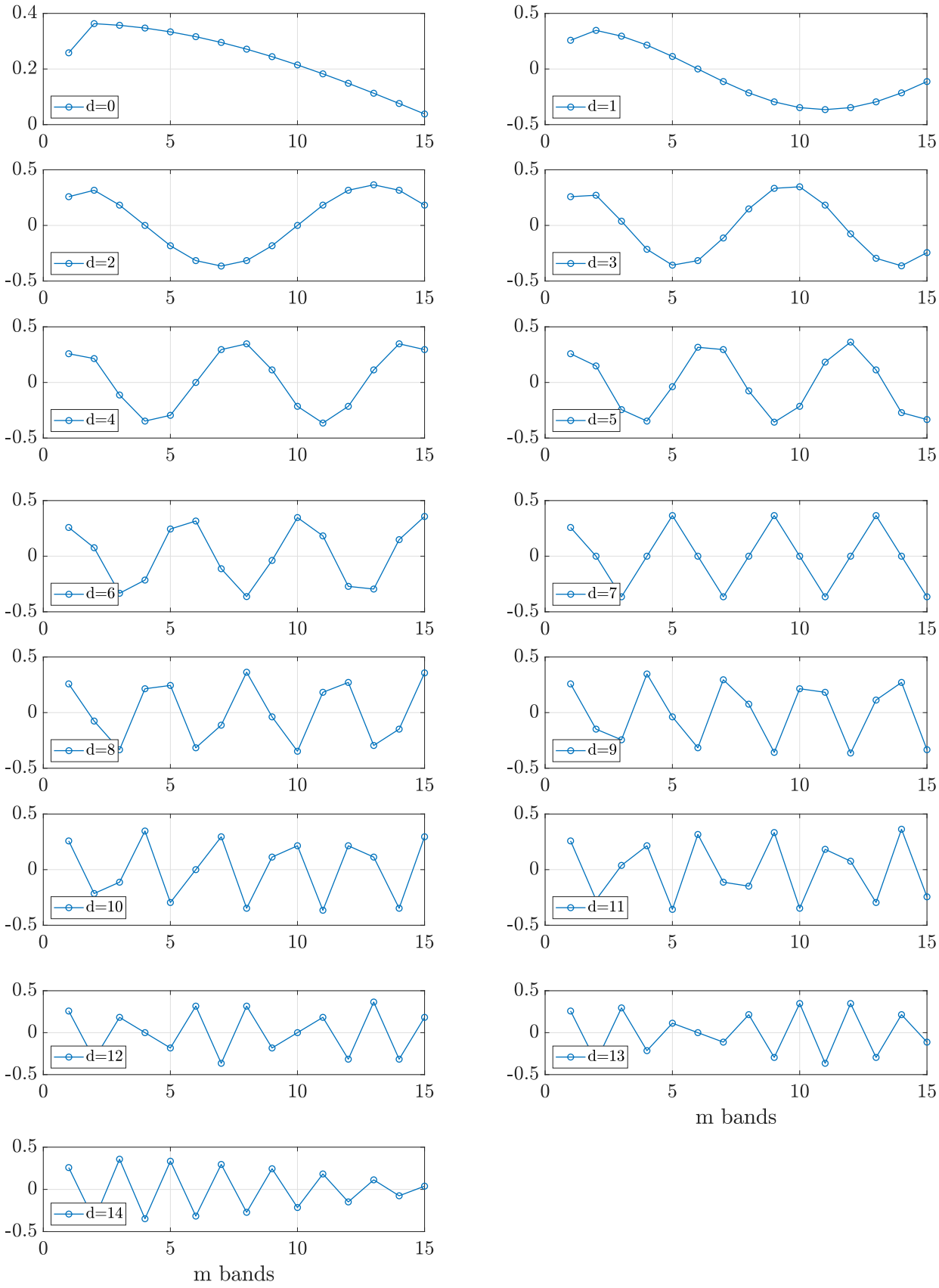

Figure 1.11: c_{IDT} Coefficients of the Inverse Discrete Cosine procedure

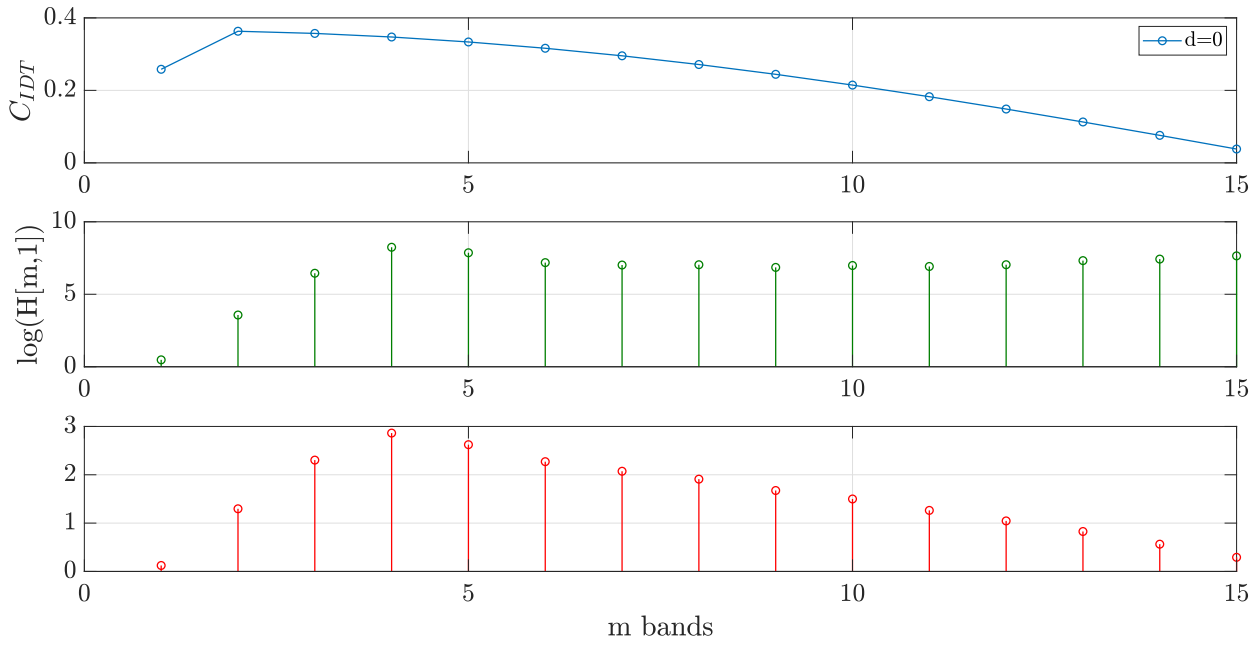

Figure 1.12: applying the discrete cosine transform coefficients to the n frame

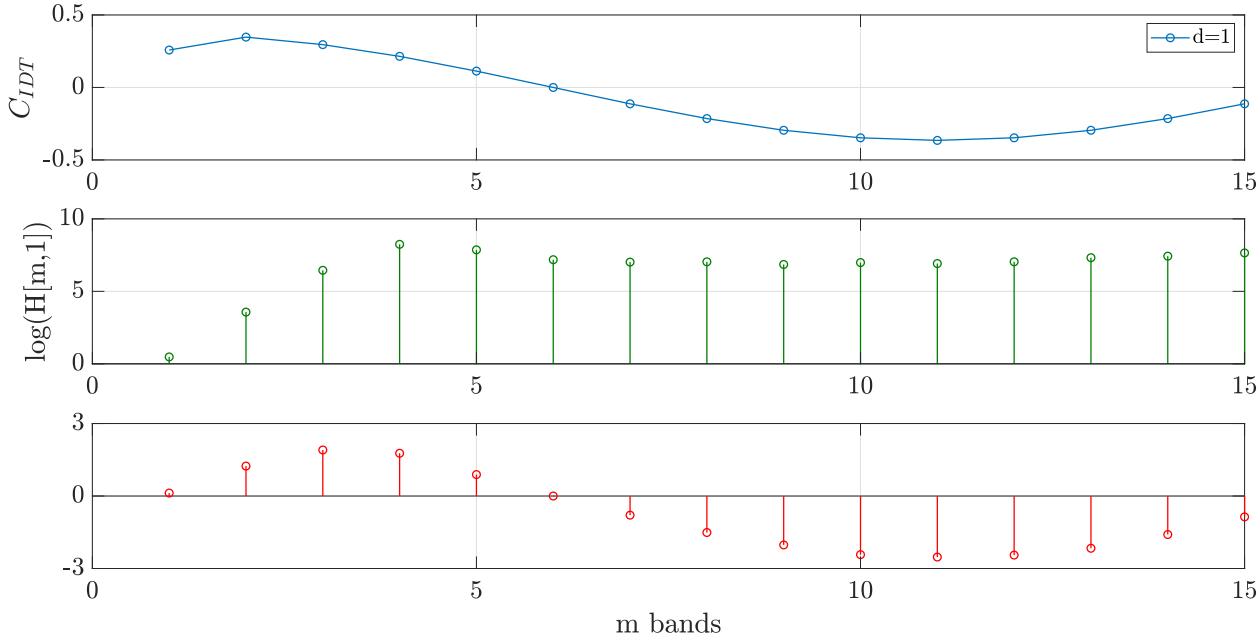

Figure 1.13: applying the discrete cosine transform coefficients to the n frame

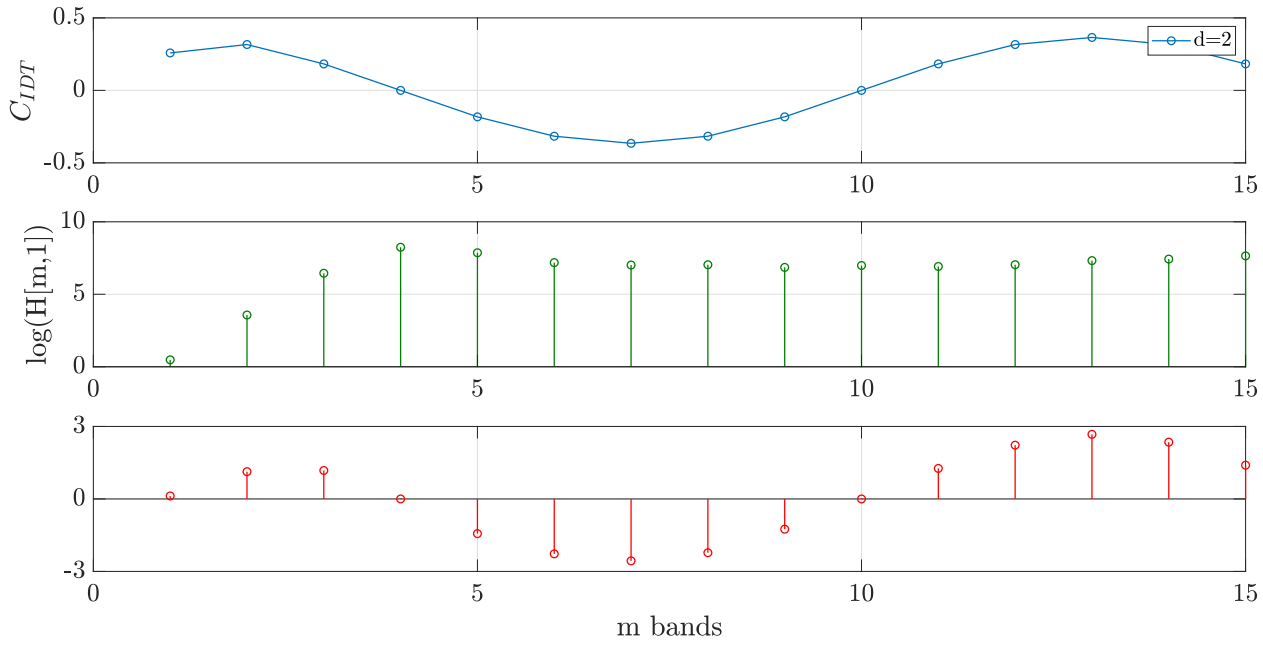

Figure 1.14: applying the discrete cosine transform coefficients to the n frame

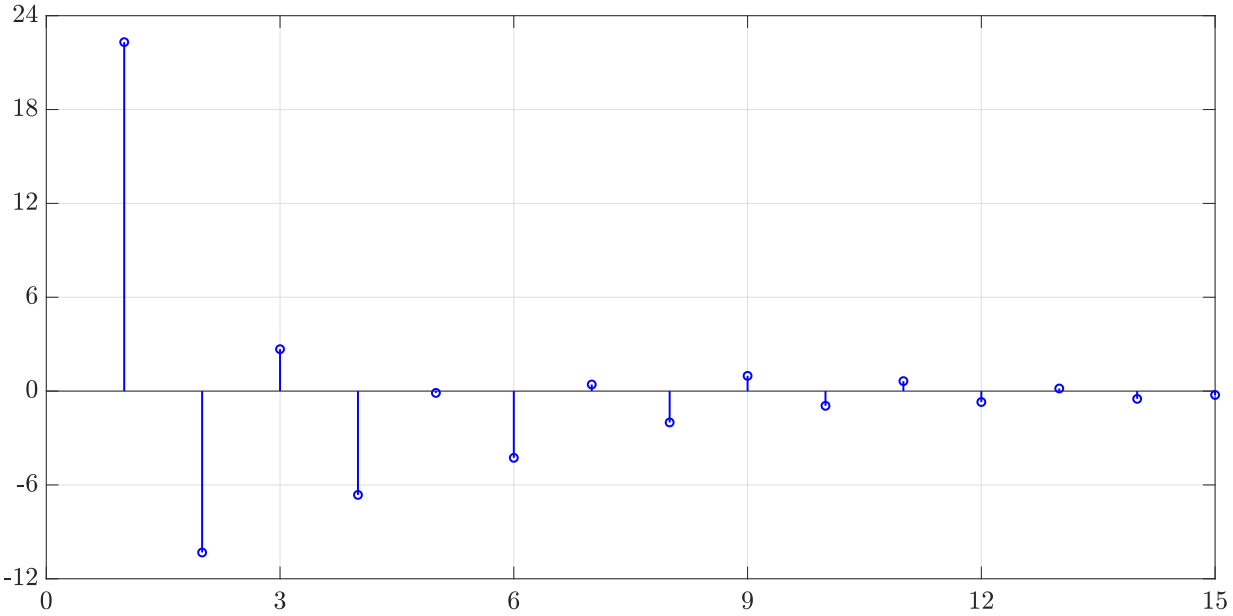

Figure 1.15: Cepstral coefficients for frame 1

Table 1.1: Cepstral Coefficients for frame 1

c_1	c_2	c_3	c_4	c_5	c_6	c_7	c_8	c_9	c_{10}	c_{11}	c_{12}	c_{13}	c_{14}	c_{15}
22,63	-10,42	2,59	-6,55	0,39	-4,14	0,51	-2,07	0,83	-1,04	0,56	-0,88	0,18	-0,49	-0,27

From this analysis, it appears that the cepstral coefficients (CCs) are always real and convey information about the physical characteristics behind the signal. For example, when $d = 0$, the cosine term of the IDCT becomes 1. Hence, the first cepstral coefficient, c_0, can be considered to represent the average power of the signal. In addition, a negative coefficient c_1 relates to the local minimum of the cosine in the IDCT noting that the higher frequency indices in the summation of the IDCT are contributing more. On the other hand, a positive peak means that there must be more power in the lower frequency range. As the number of cepstral coefficients

d becomes larger, the number of alternating partitions in the frequency range increases. For example, c_2 is a combination of the first and third partitions of the frequency scale in contrast with the second and fourth partitions. This goes on as d increases.

In this study, the inverse DCT has been used in place of inverse Discrete Fourier Transform (DFT). Defined by Ahmed et al., DCT was shown to perform better than DFT in transforming the original data into more compact and almost uncorrelated representations, and was proved to compare closely to the Karhunen-Loeve Transform (KLT), which is optimal for compressing data dimensionality. However, despite its optimality, there is no efficient algorithm able to implement KLT, while DCT may be implemented exploiting Fast Fourier Transform (FFT), i.e. in a highly computationally efficient fashion. KLT is the most basic approach to perform Principal Component Analysis (PCA), which is concerned with transforming the original data by projecting them into a reduced dimension space, whose basis vectors are represented by the data covariance eigenvectors associated with the largest eigenvalues, which, in turn, represent data components characterized by the greatest variance and are the most useful for recognition purposes.

Chapter 2

Cointegration Technique

2.1 Introduction

The current section aims to introduce the concept of cointegration and its theoretical background which is known from the econometrics literature. This section draws from a number of key texts from the econometrics literature by Johansen (1995), Fuller (1996), Maddala & Kim (1998) and Juselius (2006).

Basically, Cointegration is a mathematical method that is used, in various fields, to remove "common trends" from data sets. Recently, it has been applied to SHM studies with the purpose of identifying a feature that can only give information on the health of the structure without the effects of external distrubances [6].

2.2 Cointegration

To briefly explain the idea behind cointegration, let's start from a set of non-stationary time series, that represents the evolution of the dynamic response of the system over time. The non-stationarity of the signal could come from a variety of reasons, from damage to environmental conditions. The aim is to define a combination of such non-stationary signals that is now stationary (where the non-stationairy has been confined only to the damage) and that can be used as a damage index or control parameter.

To state a simple definition of cointegration, the following could be used:

Definition *Two or more non-stationary time series are cointegrated if a linear combination of them is stationary. If this stationary combination exists, the initial time series are defined cointegrated.*

In the following equation, where the non-stationary time series are modelled as a Vector AutoRegressive (VAR) process $\{y_i\}$ (in keeping with common practice in structural dynamics, vectors will be denoted with curved brackets $\{-\}$, and matrices with square brackets $[-]$), the series $\{y_i\}$ are cointegrated if a vector $\{\beta\}$ exists such that z_i is stationary, where

$$z_i = \{\beta\}^T \{y_i\} \tag{2.1}$$

If this is the case, $\{\beta\}^T$ is called a cointegrating vector. If $\{y_i\}$ includes a total of n variables, there may be as many as $n-1$ linearly independent cointegrating vectors. Clearly, for the time series to be cointegrated, to begin with, they must have shared/common trends.

An additional restriction that the initial non-stationary time series $\{y_i\}$ must satisfy is the following:

Definition *If a non-stationary process variable y becomes stationary after differencing d times, it is said to be integrated of order d, which is denoted* $y \sim I(d)$.
In other words, the time series must have the same "degree of non-stationarity" if they are cointegrated.

For the purposes of SHM, the intent would be to use monitored variables that are cointegrated and find the cointegrating vector to create a stationary residual sequence for damage detection. From an engineering point of view, monitored variables from the same process or system are more than likely to share common trends on account that each process variable will be driven by the same latent influences. This cannot be said, however, of the order of integration of each monitored variable, this must be ascertained before any attempt is made to find the cointegrating vector. The order of integration of a time series is ascertained in econometrics by employing a stationarity test, which is often analogous to testing for a unit root in a time-series model. The stationarity test

employed here is called the augmented Dickey-Fuller (ADF) test, the reader is referred to [7] for a detailed treatment of the subject. Once it has been ascertained to what order all process variables of interest are integrated to, it remains to find the cointegrating vector that will result in the most stationary combination of the variables.

In the context of SHM usually the reference time series are simply the dynamic features of monitored structures (eg. accelerations, frequencies, etc); thus, if it exists, the co-integration relationship will possibly be nonlinear. Here this topic is addressed considering, on one hand, the possibility of having both linear and nonlinear combinations and on the other hand, considering as reference time series, the cepstral coefficients extracted from the acceleration response of the investigated system.

Chapter 3

Simulated Cantilever Beam

3.1 Beam and analysis description

The simulated system tested is a steel cantilever beam (Fig. 3.1), modeled according to the common Euler-Bernoulli's beam theory. In this analysis, the beam is divided in 20 subelements (Fig. 3.2). The nodes are numbered in ascending order, so that the node closest to the constraint is labeled as 1. The energy dissipation properties of the system are modeled through the Rayleigh damping model. The material chosen for the beam is steel and the mechanical and geometric properties assigned to the beam are reported in Table (3.1)

In this analysis, we are also investigating the effect of temperature on the estimation of the cepstral coefficients. This is because the effects of temperature variation could induce the alteration in the values of the cepstral coefficients similar to those induced by structural damage and so it is important to study these effects and find ways to eliminate them. Here, in the beam example, the mechanical parameters are considered to be temperature-dependent according to the following expressions.

$$L = L_0(1 + \alpha\Delta T)$$
$$A = A_0(1 + \alpha\Delta T)^2$$
$$I = I_0(1 + \alpha\Delta T)^4$$
$$\rho = \frac{\rho_0}{(1 + \alpha\Delta T)^3}$$
$$E = E_0(1 + \beta\Delta T)$$

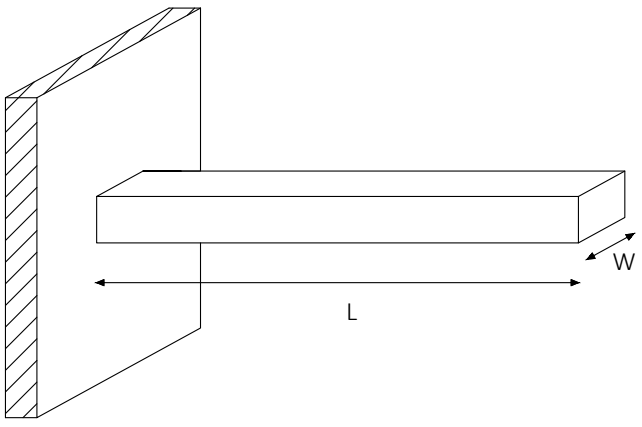

Figure 3.1: Cantilever Beam

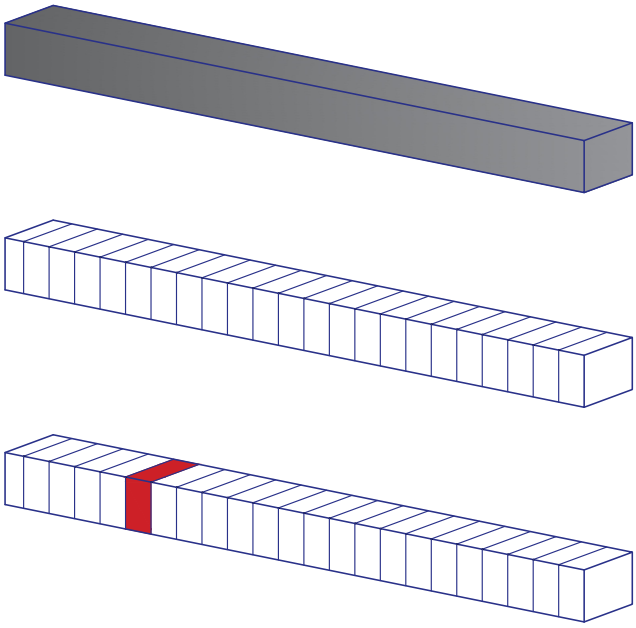

Figure 3.2: Cantilever Beam

Table 3.1: Mechanical and geometric properties

Mechanical Property	Symbol	Value
Length	L[m]	5
Section Height	H[m]	0.3
Section Base	B[m]	0.3
Young's Modulus	E[GPa]	210
Volume Density	$\rho[\frac{kg}{m^3}]$	8000

In order to test the capability of the cepstral coefficients to detect structural damage from the analysis of the beam's response, a "damaged" beam has also been considered. The damage condition is simulated introducing a reduction of 10 % of the stifness of the 6^{th} subelement (Fig. 3.2).

To consider operational conditions with different temperature, so to simulate the working conditions of a bridge during different seasons, two different set of simulations are run for the cantilever beam: a set of 4500 simulations considering the system in its healthy state and another set of 3600 tests in which the beam is defined damaged. Each one of these simulations, both in the undamaged or damaged conditions, corresponds to a specific value of temperature. In each simulation the acceleration response to a white Gaussian noise input is simulated. The input time history, of mean 0 and standard deviation 1, is 2 minutes long with sampling frequency of 200 Hz and it is applied at the free node of the beam. The response is simulated applying the Newmark integration approach. An additional 10 % noise is added to the computed values of the acceleration response of the beam so to include the effect of measurement noise in the inverse analysis.

A matrix collecting the cepstral coefficients time history for each sensor is extracted following the procedure presented in Chapter 1. In order to have only one vector of coefficients for each observation the extracted vector are averaged over the frames. The 15 cepstral coefficients extracted for the first sensor in the undamaged condition, together with the simulated temperature variation, are presented in Fig.3.3 and Fig.3.4. Comparing the behavior of the cepstral coefficients with the simulated variation of temperature, it can be noticed how some of the coefficients are influenced by the environmental fluctuations (c_1, c_2, c_3), while others remain mainly stationary (c_4, c_6, c_7). The same behavior can be observed for the coefficients computed from the time histories measured with the other 19 sensors.

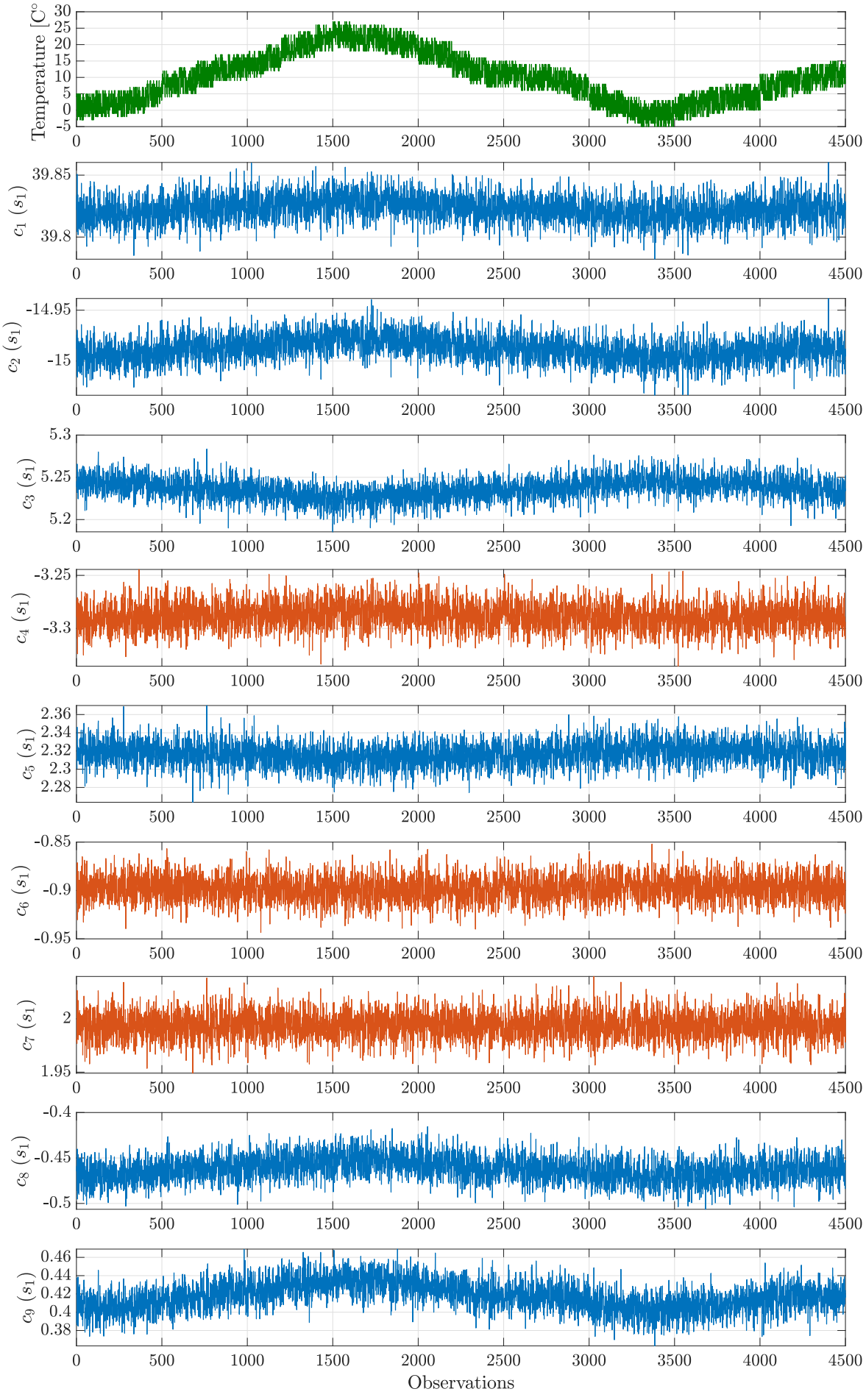

Figure 3.3: Temperature variation and CC 1-9 for sensor 1 in undamaged conditions

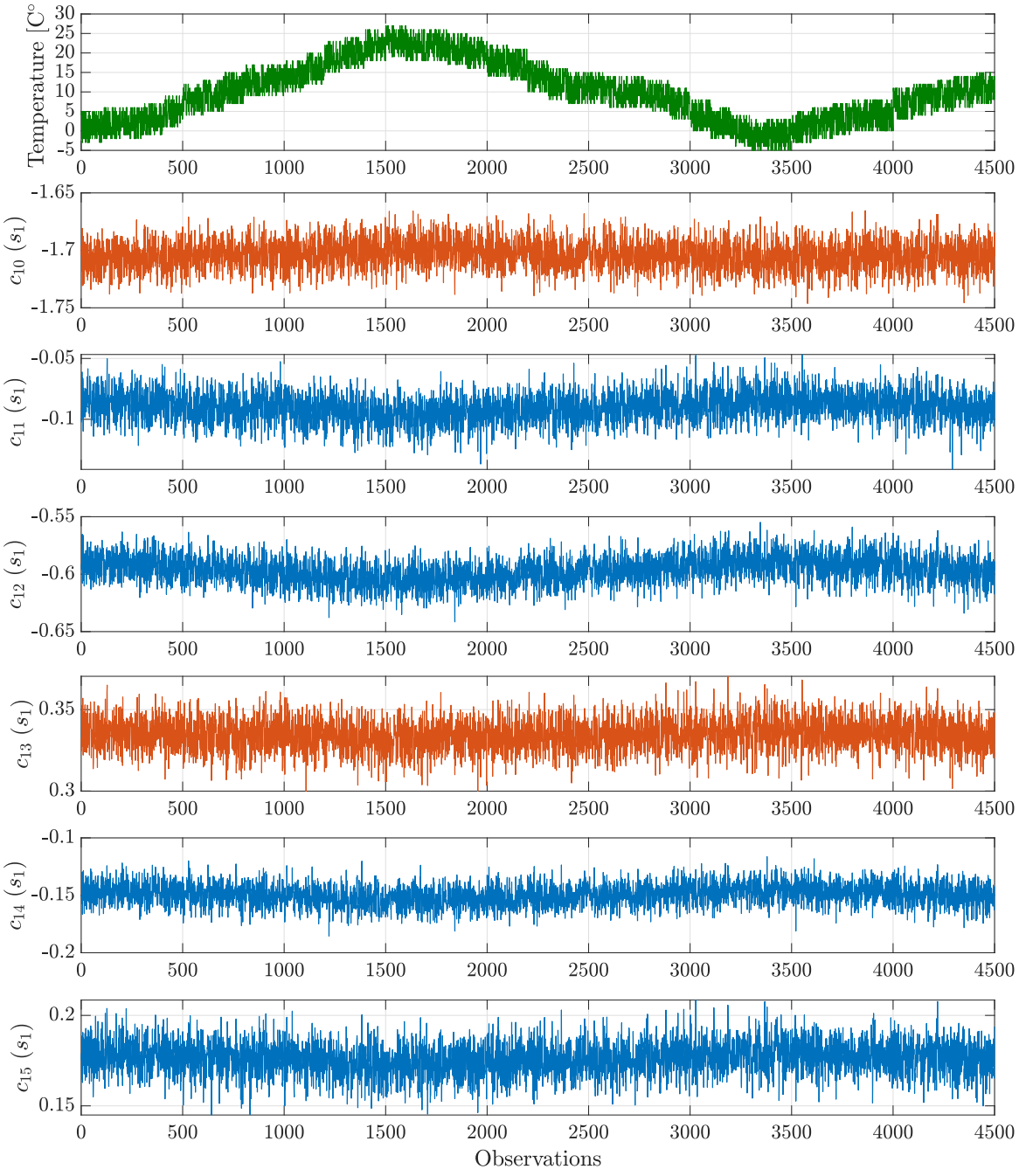

Figure 3.4: Temperature variation and CC 10-15 for sensor 1 in undamaged conditions

The corrispondent cepstral coefficients for the damaged conditions are presente din Fig.3.5 and Fig.3.6 where the occurrence of damage is indicated by the vertical red line. The jump due to the change in stiffness is more visible in the first cepstral coefficients, while it tends to fade in the last features.

In the time histories of coefficients affected by the variation of temperature, this little gap presents the same magnitude order of the fluctuations due to temperature and because of that the damage could be hidden and not detected. In the stationary coefficients, instead, the presence of damage clearly shows up.

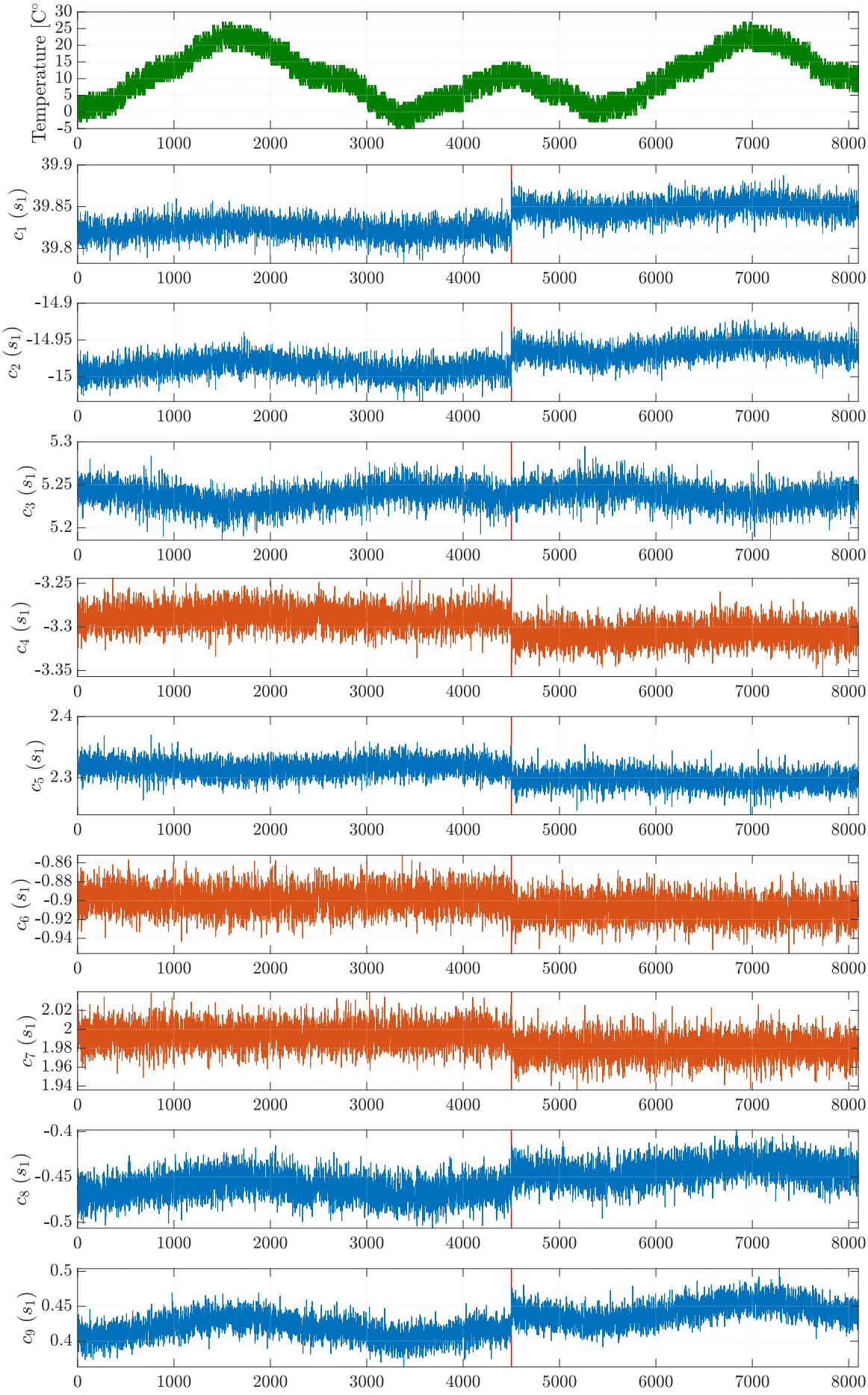

Figure 3.5: Temperature variation and CC 1-9 for sensor 1 in damaged conditions

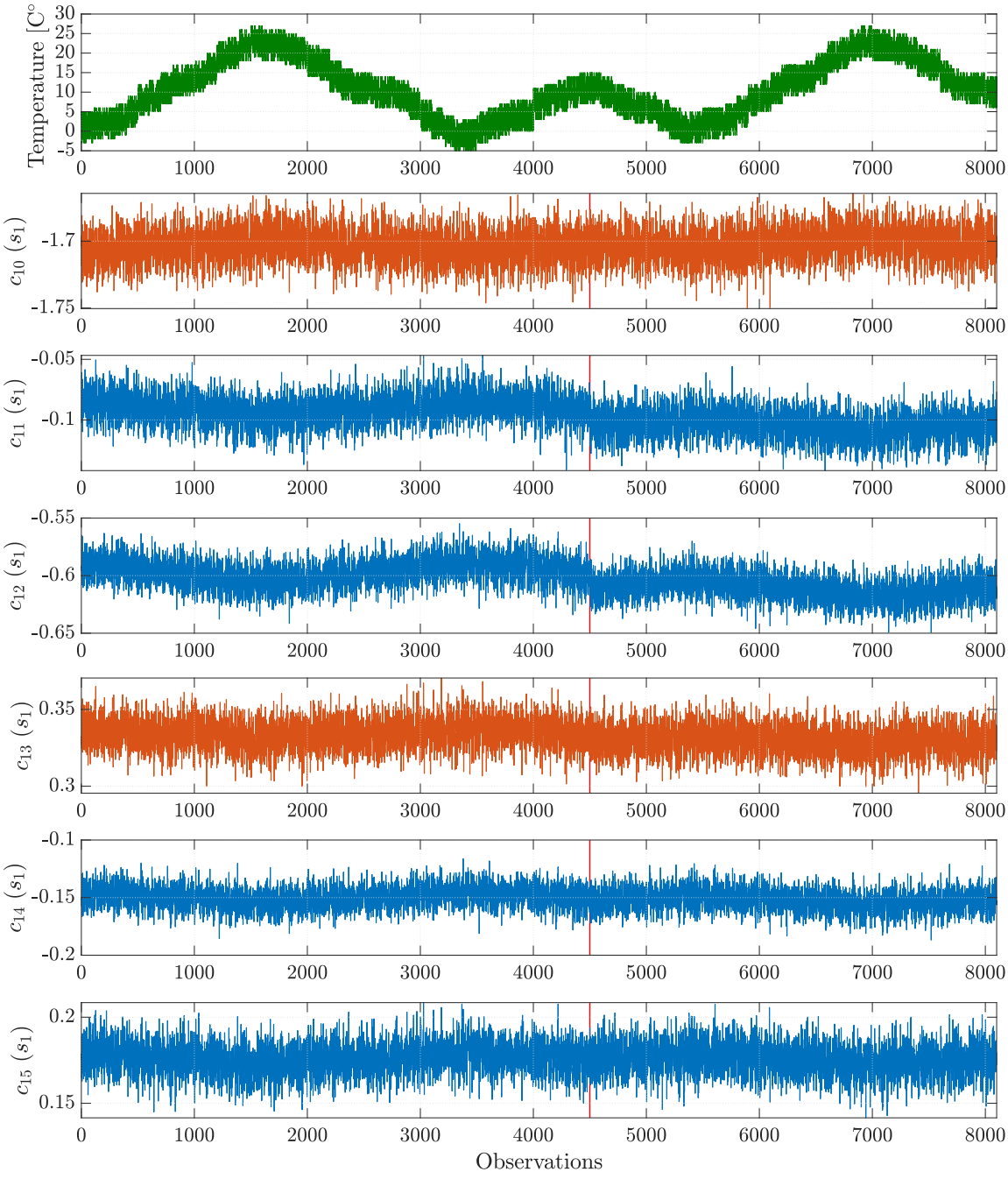

Figure 3.6: Temperature variation and CC 10-15 for sensor 1 in damaged conditions

3.2 Application of Cointegration Technique to beam data

To separate the temperature effects from the damage effects, the cointegration presented in this section is carried out considering the Support Vector Machine method for the computation of the cointegrating vector. This methodology is implemented considering a Gaussian Kernel and 10 Folds for the Cross Validation. The model is trained over the a training specimen of 1500 data from observation 1000 until 2500 which is the range of data that consider the wider variation of temperature affecting the beam.

The application of the cointegration technique on the cepstral coefficients affected by the temperature variation leads to the combined residual regression which is stationary and detrended (Fig.3.7 and Fig.3.8). This procedure allows to highlight the occurrence of damage in a clearer fashion. In a simple case like this simulated beam the damage, even if extremely small, could be spotted as well just looking at the cepstral coefficients not affected by the environmental fluctuations.

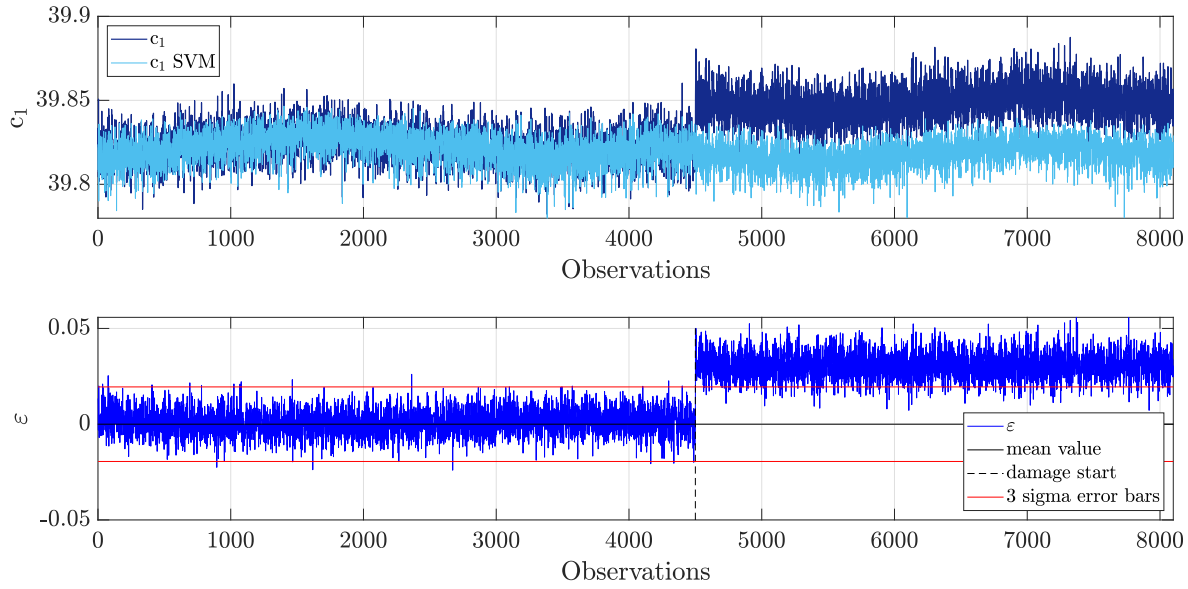

Figure 3.7: Timehistory of Cepstral Coefficient 1, the coefficients SVM regression and the residuals between them

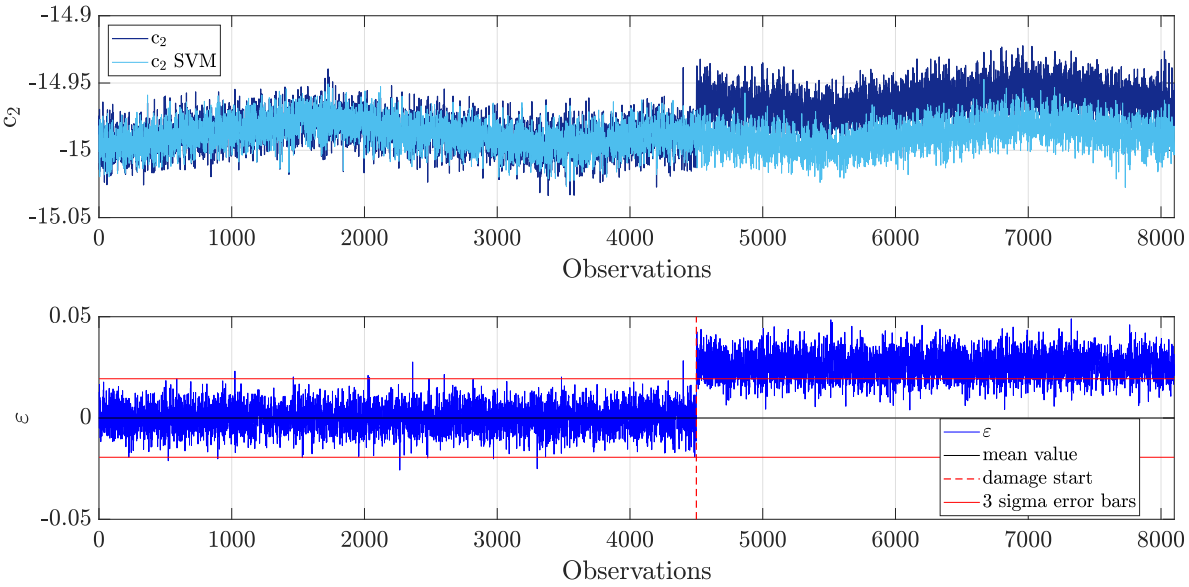

Figure 3.8: Timehistory of Cepstral Coefficient 2, the coefficients SVM regression and the residuals between them

Chapter 4

Z24 Bridge

Here, we discuss the results about the extraction of the cepstral coefficients and the application of the cointegration technique from data recorded on a real structure, the Z24 bridge, that was subjected to an extensive monitoring campaign before being demolished. The Z24 bridge tests described here have been performed within the European Brite EuRam research project BE-3157, "System Identification to Monitor Civil Engineering Structures" (SIMCES).

One of the main objectives of the SIMCES project was to deliver a proof of feasibility for vibration-based structural health monitoring of civil engineering structures by full-scale, long-term tests and progressive failure tests of a representative structure, the Z24 Bridge. The project was coordinated by Katholique University of Leuven (Department of Civil Engineering, Structural Mechanics Section).

4.1 Bridge Description

Figure 4.1: Views of the Z24 bridge

The Z24 bridge was a post-tensioned concrete two-cell box-girder bridge located in Switzerland, in the Bern canton near Solothurn. It was built in 1963 and it connected the villages of Koppigen and Utzenstorf, overpassing the A1 highway between Bern and Zurich. The bridge presented a main span of 30 m and two side spans of 14 m (Fig.4.2).The bridge was built as a free standing frame with the approaches backfilled later. Both abutments consisted of triple concrete columns connected with concrete hinges to the girder. Both intermediate supports were concrete piers clamped into the girder. An extension of the bridge girder at the approaches provided a sliding slab. The bridge was slightly skew because all supports were rotated with respect to the longitudinal axis. The bridge was demolished at the end of 1998, because a new railway next to the highway required a bridge with a larger side span.

A year before the demolition, a long-term environmental monitoring system (EMS) was installed and the bridge was monitored from 11 November 1997 till 11 September 1998. The final goal of this monitoring test was to provide both environmental and response vibration data of the bridge, in order to subsequently quantify the contribution of the environmental fluctuations on the bridge dynamics. The EMS consists in the installation of different sensors to measure different environmental parameters: air temperature, air humidity, rain true or false, wind speed, and wind direction. Also a sensor consisting of two inductive loops was installed to detect the presence of vehicles on the bridge. Particular attention was given to the temperature factor. At the middle of the three spans, the temperature was measured at eight points on the girder: at the center of the north

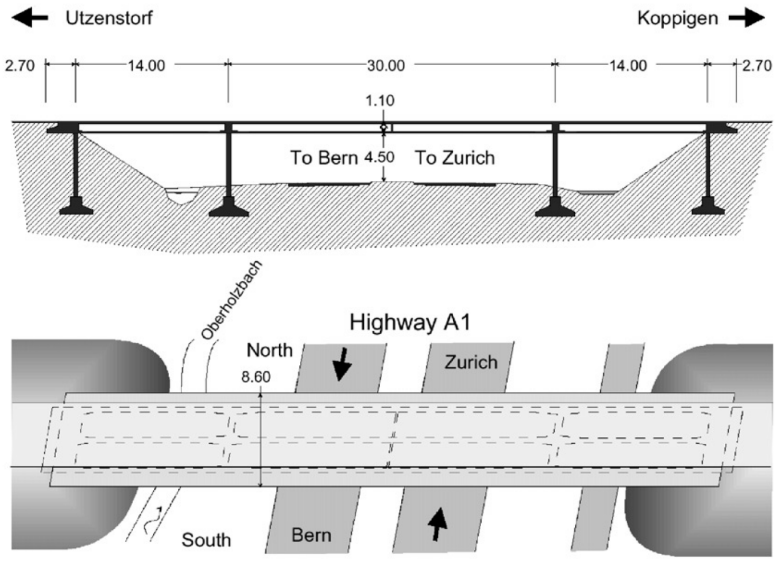

Figure 4.2: Bridge section and plan view

(TWN), central (TWC), and south (TWS) web; below the north (TSWN) and south (TSWS) sidewalk; at the top (TDT) and soffit (TDS) of the deck, and at the soffit (TS) of the girder. The soil temperature near each of the concrete columns at the approaches was monitored, as well as that near the north, central, and south parts of the intermediate piers (12 sensors in total). Although the original blueprints of the Z24 bridge indicated that the asphalt layer should have a thickness of 5 cm, the drilling of access holes for the installation of the temperature sensors on the girder revealed a cover of 16-18 cm of asphalt. Therefore, the temperature of the pavement (TP) was measured at the middle of the three spans.

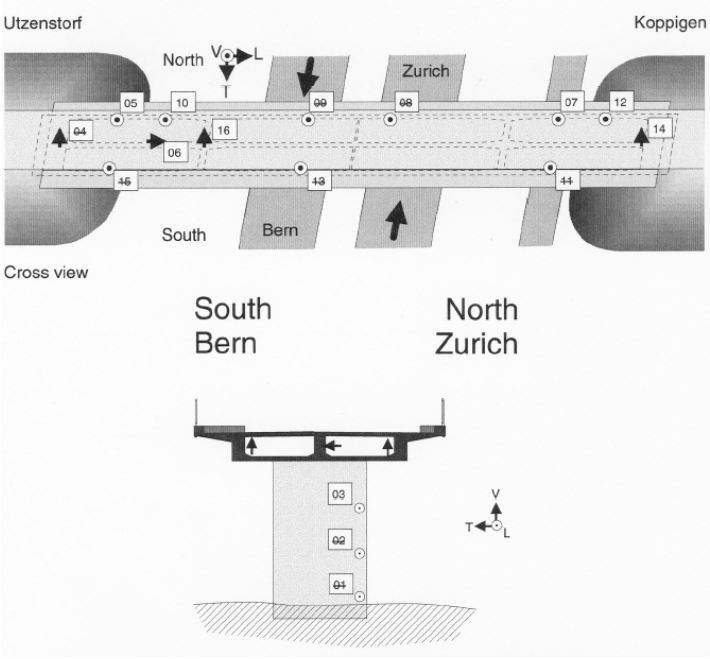

Figure 4.3: Sensors location

To monitor the bridge dynamics, the structural acceleration was measured at 16 locations on the bridge in different directions. Every hour, 10 scans of environmental data, sampled at 48 sensors, and 8 averages of 8192 acceleration samples, taken at the 16 sensors, were collected and stored to a hard disk after compression. The construction works at the new bridge that replaced the Z24, caused the loss of six temperature sensors and damage to one accelerometer. Although the type of accelerometers that had been used was specially designed for long-term use, some showed a considerable drift and a few of them failed during operation.

A series of progressive damage tests have been carried out during the summer of 1998, shortly before complete demolition of the bridge. The first eight scenarios are summarised in Table 4.1. The practical significance of these tests was ensured by checking that they were relevant for the safety of the bridge and that the simulated damage occurred frequently. The settlement is simulated by cutting the Koppigen pier and removing about 0.4m of concrete. Lowering and lifting was done by six hydraulic jacks. During the tests, the pier rested on steel sections with similar stiffness as the uncut concrete section. Other damage scenarios (spalling of concrete, landslide, cut of concrete hinges, failure of anchor heads, rupture of tendons) are not considered here as they caused no or a minor degradation of bending stiffness.

Figure 4.4: Damage scenarios

With a measurement grid consisting of a regular 3 × 45 grid on top of the bridge deck and a 2 × 8 grid on each of the two pillars, 291 degrees of freedom have been measured: all displacements on the pillars, and mainly vertical and lateral displacements on the bridge deck. Because the number of degrees of freedom to be measured exceeded the number of available accelerometers and acquisition channels, the data were collected in nine setups using five reference channels. The forced excitation was applied by two vertical shakers, placed on the bridge deck. A 1 kN shaker was placed on the middle span and a 0.5 kN shaker was placed at the Koppigen side span. The shaker input signals were generated using an inverse fast Fourier transform (FFT) algorithm, resulting in a fairly flat force spectrum between 3 and 30 Hz. After scenario 8, a drop weight test was also performed, using a device that allowed to drop a mass of up to 120 kg from a height of up to 1 m in a controlled way. The applied shaker and drop weight forces were periodic with eight periods. A total of 65536 samples was collected at a sampling rate of 100 Hz, using an antialiasing filter with a 30-Hz cutoff frequency.

Table 4.1: Damage Scenarios on Z24

♯	Date	Scenario
1	04/08/1998	Undamaged condition
2	09/08/1998	Installation of pier settlement system
3	10/08/1998	Lowering of pier, 20 mm
4	12/08/1998	Lowering of pier, 40 mm
5	17/08/1998	Lowering of pier, 80 mm
6	18/08/1998	Lowering of pier, 95 mm
7	19/08/1998	Lifting of pier, tilt of foundation
8	20/08/1998	New reference condition
9	25/08/1998	Spalling of concrete at soffit, 12 m^2
10	26/08/1998	Spalling of concrete at soffit, 24 m^2
11	27/08/1998	Landslide of 1 m at abutment
12	31/08/1998	Failure of concrete hinge
13	02/09/1998	Failure of 2 anchor heads
14	03/09/1998	Failure of 4 anchor heads
15	07/09/1998	Rupture of 2 out of 16 tendons
16	08/09/1998	Rupture of 4 out of 16 tendons
17	09/09/1998	Rupture of 6 out of 16 tendons

4.2 Extraction of the Cepstral Coefficients

The cepstral coefficients are computed according the procedure presented in Chapter 1. The response measurements are detrended before extracting the cepstral coefficients and there is no additional manipulation of the time histories. One vector of coefficients is computed for each frame in which every single time history (observation) is decomposed. In order to have only one vector of coefficients for each observation, the extracted vector are averaged over the frames.

The cepstral coefficients extracted from the Z-24 bridge acceleration measurements appear to be quite noisy and their variability is quite high (Fig. 4.5); nevertheless, it is possible to underline some trends in the data. In order to overcome this variability a simple moving average is introducted (Fig. 4.6) and the averaged coefficients are adopted as the new features. This procedure is implemented considering 20 samples as the number of previous data points to be used in conjunction with the current data point when calculating the moving average.

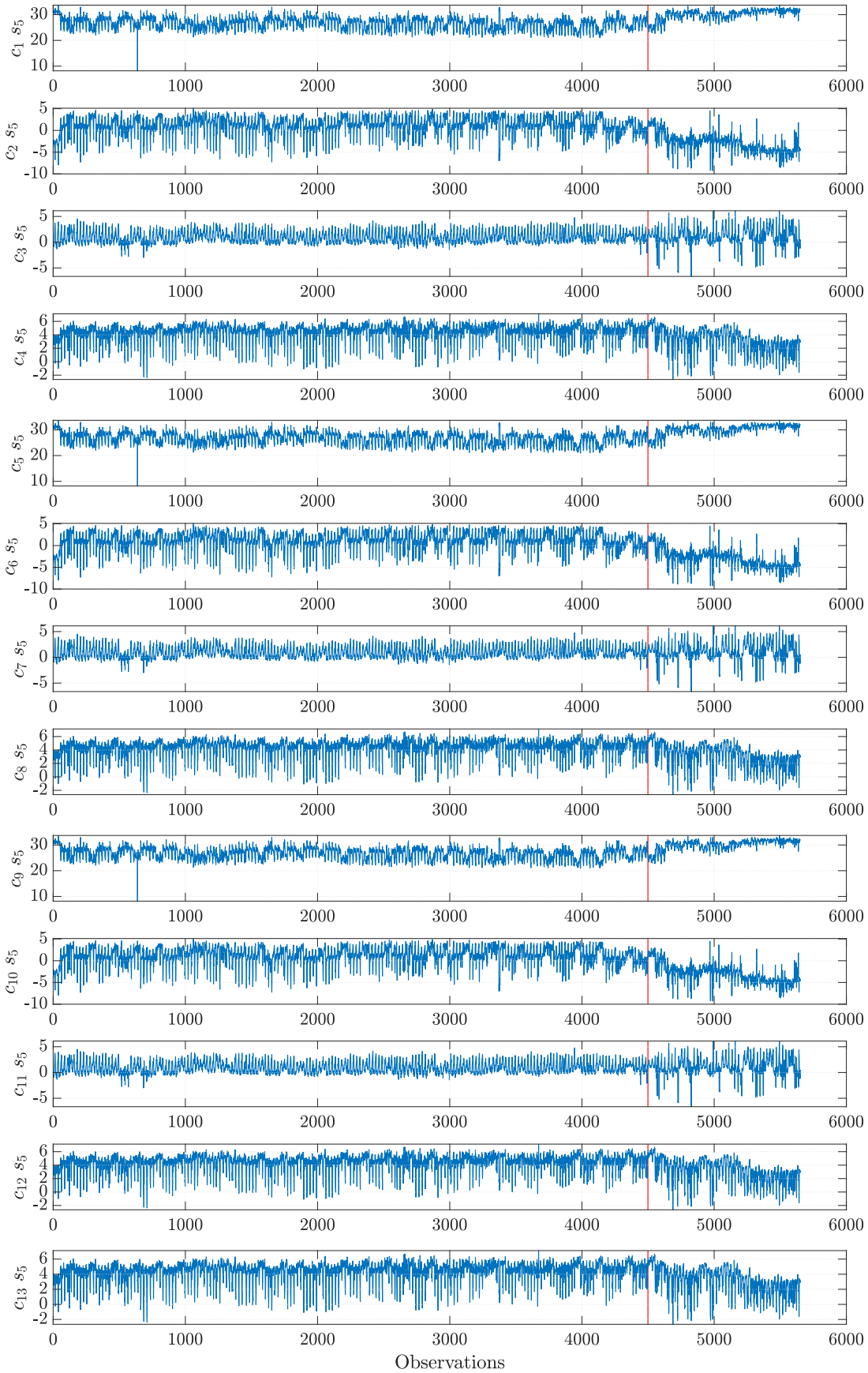

Figure 4.5: Cepstral coefficients extracted for sensor 5

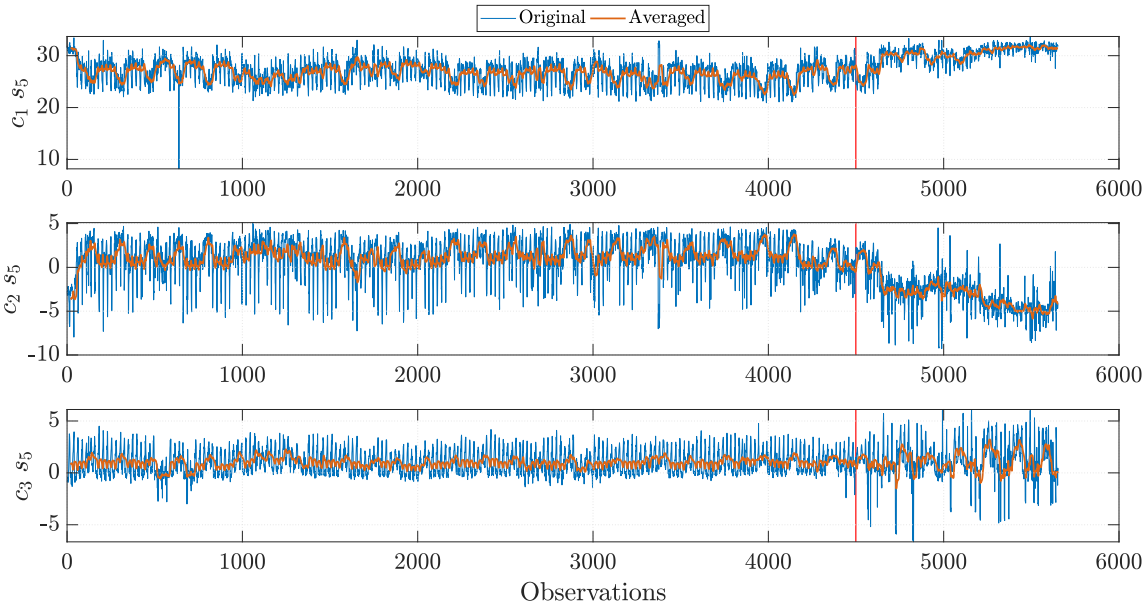

Figure 4.6: Cepstral coefficients with and without moving average

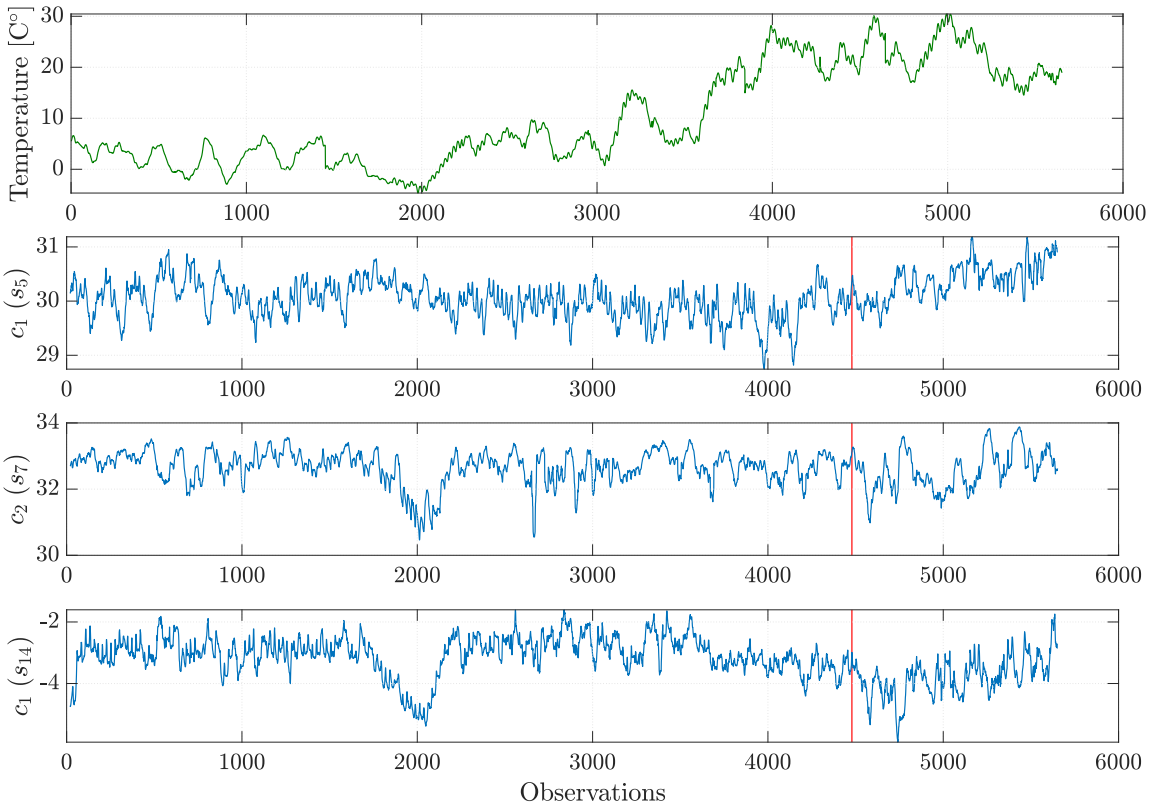

Figure 4.7: Temperature Observations and examples of cepstral coefficients for different sensors

Comparing the temperature variation with the time history of the cepstral coefficients, it can be noticed that some of the coefficients are quite insensitive to the environmental fluctuations (c_1 (s_1)); while others (c_2 (s_7) and c_1 (s_{14})) shows clearly a match with the temperature drop around the 2000^{th} observation (Fig.4.7).

The variation due to the environmental conditions and the one caused by the introduction of damage (damaged starts after the red line) are comparable and consequently, the presence of damage can be hidden. This is an important observation because it could impair the effectiveness of the damage assessment procedure. It is in this case that the cointegration technique could be extremely helpful, in this real tests, in removing any trend in the data induced by environmental data and highlighting instead the variations induced by damage.

4.3 Cointegration procedure to remove environmental effects

The cointegration presented in this section is carried out considering the Support Vector Machine method for the computation of the cointegrating vector. This methodology is implemented considering a Gaussian Kernel and 10 Folds for the Cross Validation. The model is trained over a specimen of 1000 data points. The data are normalized and the coefficients are considered with their absolute value.

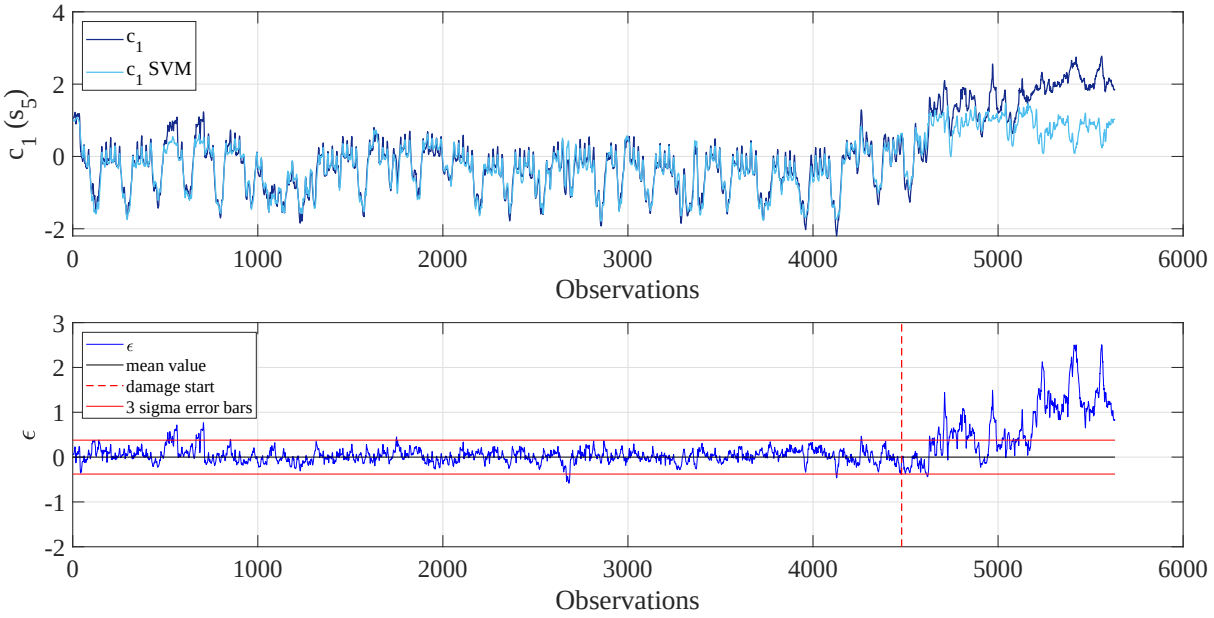

Figure 4.8: Time history of Cepstral Coefficient 1 for sensor 5, the coefficients SVM regression and the residuals between them

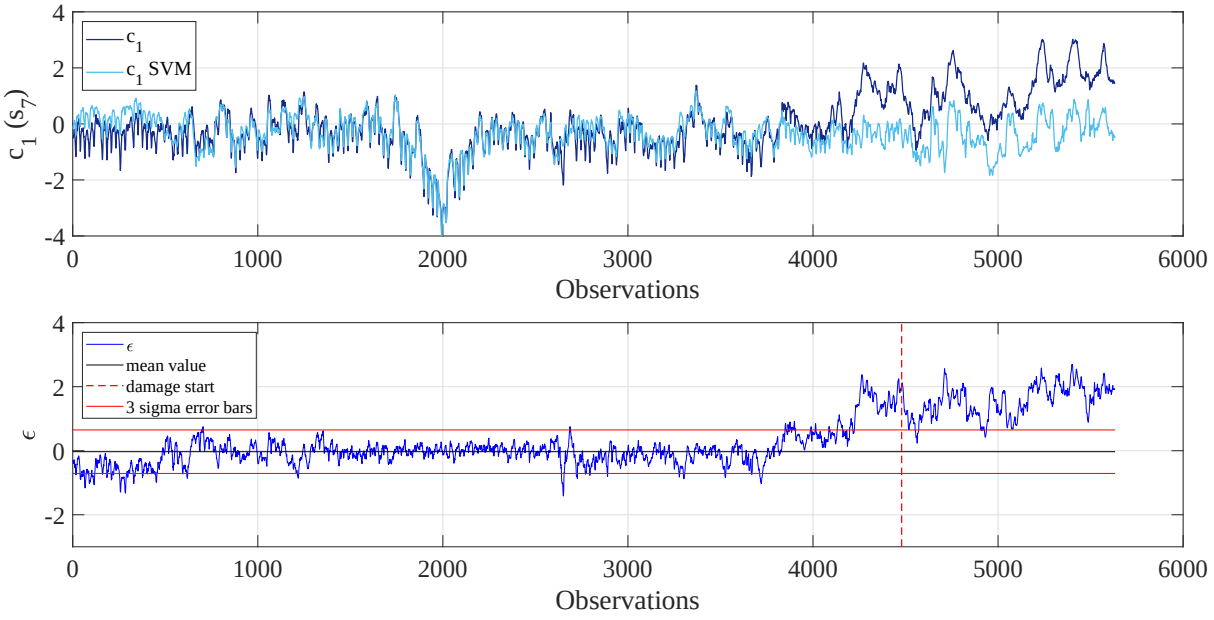

Figure 4.9: Timehistory of Cepstral Coefficient 1 for sensor 7, the coefficients SVM regression and the residuals between them

From the analysis of the residuals, it is clear the appearance of the structural damage while the fluctuations induced by temperature variations have been removed. In fact, it is only after the red dotted line (corresponding to the occurrence of damage) that the residuals between cointegrated cepstral coefficients show a clear departure from the 3 standard deviation error band. The application of the cointegration technique on the cepstral coefficients in this real case is indispensable to detect the damage; particularly for the coefficients for which the damage presents the same magnitude variation of environmental fluctuations (Fig. 4.9). Applying this

procedure the damage is well identified and the residuals coming from time histories with environmental trends are totally cleaned up.

Chapter 5

Conclusions

In this report, the results of an study investigating the possibility of using a speaker recognition approach to structural health monitoring have been presented. In particular, this study focused on the use of particular features used in speaker recognition (Frequency Warped Cepstral Coefficients) as damage sensitive features and on the effects that environmental conditions can have on such coefficients. In fact, it is a well known problem in monitoring the infrastructure system that the effects of temperature could alter the dynamic characteristics (e.g. natural frequencies) of a bridge up to 10% and this could hide the occurrence of structural damage.

The framework used in this study follows within the category of "Pattern Recognition" approach. The basic idea behind such methods is to monitor the variational pattern of certain features (e.g. natural frequencies, mode shapes, etc.) extracted from the measured structural response. The performance of these approaches predominantly depends on how well these features reflect the actual condition of the structure. In fact, modal parameters, such as natural frequencies and mode shapes are commonly used in monitoring the performance of bridges and buildings: however, in assessing the damage of such structures, these features could be misleading in pointing out the integrity status of the structure since they are highly influenced by the usual fluctuations in environmental and operational conditions. The effects of environmental and operational conditions could overshadow the occurrence of deterioration and damage, invalidating the purpose of the investigation.

In this study, an adaptation of Mel-Frequency Cepstral Coefficients as damage sensitive features for structural health monitoring of civil structures was addressed. Typically used in speaker recognition methodologies, these indices offer an extremely easy extracting process with a few user-defined parameters and a low computational burden and they have been shown to be an effective alternative to other features for damage detection problems. To remove environmental effects from the coefficient estimation, a technique called "Cointegration", quite popular in econometrics, has been applied. Two study cases were presented: 1) a numerical simulation of a cantilever beam subject to environmental variations both in undamaged as well as damaged conditions, and 2) the benchmark case of the Z24 bridge, a structure in Switzerland that was recently demolished and that was fully instrumented, during operational conditions as well as during demolition.

From the results of this study, it appears that the following conclusions can be drawn: 1) the cepstral coefficients have the potential to become quite useful damage sensitive features that can be used on bridge structures: they are compact features, easy to obtain, and require little input from the user, and 2) the cointegration technique appears to be a very effective technique to remove non-stationary effects such as those induced by the environment temperature. As shown in this report, the analyses conducted on data from the tests run on the Z24 bridge show great potential for both techniques and and warrants further investigation.

Bibliography

[1] B.P.Bogert, M.J.R.Healy, J.W.Tukey, The quefrency alanysis oftimeseries for echoes: cepstrum, pseudoautocovariance, cross-cepstrum and saphecracking, M.Rosenblatt(Ed.), *Proceedings of the Symposium on Time-Series Analysis*, vol.15, Wiley, New York 1963, pp.209–243.

[2] A.V.Oppenheim, R.B.Schafer, *Discrete Time Signal Processing*, Prentice–Hall, Englewood Cliffs, NJ, 1989.

[3] S.B. Davis, P. Mermelstein, Comparison of parametric representations for monosyllabic word recognition in continuously spoken sentences, *IEEE Transactions of Acoustic, Speech, SignalProcessing* 28 (4)(1980)357–366.

[4] G.Zhang, R.S. Harichandran, P. Ramuhalli, Application of noise cancelling and damage detection algorithms in NDE of concrete bridge decks using impact signals, *Journal of Nondestructive Evaluation* 30 (4)(2011)259–272.

[5] L. Balsamo, R. Betti, H. Beigi, A structural health monitoring strategy using cepstral features, *Journal of Sound and Vibration* 333 (2014) 4526–4542.

[6] E. J. Cross, K. Worden, Q. Chen, Cointegration: a novel approach for the removal of environmental trends in structural health monitoring data, *Proceeding of the Royal Society A* 467 (2011), 2712–2732.

[7] D. A. Dickey, W. A.Fuller, Distribution of the estimators for autoregressive time series with a unit root, *Journal of the American Statistical Association* 74 (1979), 427–431.